Comparison of ocean heat content estimated using~~from~~ two eddy-resolving hindcast simulations ~~using~~ based on OFES1 and OFES2

Fanglou Liao[1,2], Xiao Hua Wang[2*], and Zhiqiang Liu[1,3*]

[1]Department of Ocean Science and Engineering, Southern University of Science and Technology, Shenzhen, 518055, China
[2]The Sino-Australian Research Consortium for Coastal Management, School of Science, The University of New South Wales, Canberra, 2610, Australia
[3]Southern Marine Science and Engineering Guangdong Laboratory (Guangzhou), Guangzhou, 511458, China

Correspondence to: Zhiqiang Liu (liuzq@sustech.edu.cn) or Xiao Hua Wang (x.h.wang@unsw.edu.au)

Abstract. ~~The~~ In this study, we have compared the ocean heat content (OHC), ~~estimates~~ estimated ~~from~~ using two eddy-resolving hindcast simulations ~~from~~ based on ~~the~~ Ocean General Circulation Model for the Earth Simulator Version 1 (OFES1) and Version 2 (OFES2)~~ and~~. Results from a global objective analysis of subsurface temperature ~~observations~~ (EN4)~~,~~ were taken as a reference. Both EN4 and OFES1 suggest that OHC has increased ~~above 2000 m~~ in most regions of the ~~global ocean~~top 2000 m ~~above 2000 m in the EN4 and OFES1 over~~ during 1960–2016, ~~mainly due~~~~a result to~~which is mainly associated with~~of~~ the deepening of neutral density surfaces~~, with~~ and variations along the neutral density surfaces of regional importance. Upon comparing the results obtained from the two OFES hindcasts, ~~We~~ we found substantial differences in the temporal and spatial distributions of the OHC ~~between the two OFES hindcasts~~, especially in the Atlantic Ocean. A basin-wide heat budget analysis showed that there was less surface heating for the major basins in the OFES2. The horizontal heat advection was ~~largely~~ mostly similar, ~~but~~ however, the OFES2 had a ~~much~~ significantly stronger meridional heat advection associated with the Indonesian Throughflow (ITF) above 300 m. Additionally~~Also~~, large discrepancies in the vertical heat advection ~~based on the two OFES data~~ were also ~~identified~~evinced when the two OFES results were compared, especially at ~~the~~ a depth of 300 m in the Indian Ocean. We inferred that there are~~exist~~ large discrepancies in the vertical heat diffusion (cannot be directly ~~diagnosed~~ evaluated in this study~~paper~~ due to data unavailability), which, along with the different magnitudes of sea surface heat flux and vertical heat advection, were the major factors responsible for the examined ~~OHC~~ differences in OHC. This work~~works~~ suggests that ~~the~~ OFES1 provides a reasonable multi-decadal estimate of global and basin-integrated warming trends above 700 m, ~~with the exception~~~~exceptions of~~except for~~in~~ the top 300 m ~~of~~ for the Pacific Ocean and between 300–700 m ~~in~~ for the Indian Ocean. ~~Despite an exceptional agreement with~~Although ~~observations in~~ the estimates of the global OHC ~~estimate of~~during 1960–2016 are consistent with observations between 700–2000 m, caution is warranted ~~when~~ while examining the basin-wide multi-decadal OHC variations ~~by~~ using ~~the~~ OFES1. The seemingly suboptimal OHC~~,~~ estimate~~d from~~ ~~using~~based on ~~the~~ OFES2, ~~reminds us~~suggests that any conclusions on long-term climate variations derived from ~~the~~ OFES2 ~~may~~ might suffer from large drifts, necessitating audits ~~and need to be carefully audited~~.

1 Introduction

The global oceans ~~has stored~~ store ~~over~~ more than 90% of ~~the~~ extra heat that has been added to the Earth ~~system~~ since the 1950s~~5~~, ~~causing~~ generating a significant OHC increase ~~in the ocean heat content (OHC)~~ (Levitus et al., 2012; IPCC 2013). ~~The~~ Therefore, OHC ~~is therefore~~forms an important indicator of climate change~~,~~, and it ~~provides useful bounds forin~~ helps ~~estimating~~ estimate the Earth's energy imbalance (Palmer et al., 2011; Von Schuckmann et al., 2016). Although natural factors such as ~~the~~ El Niño–Southern Oscillation (ENSO) and volcanic eruptions can ~~affect~~ modulate the OHC (Balmaseda et al., 2013; Church et al., 2005), the recent warming trend has been ~~mostly~~ largely ~~resulted from~~induced by the accumulation of greenhouse gas~~gases~~ ~~accumulationaccumulating~~ in the atmosphere (Abraham et al., 2013; Gleckler et al., 2012; Pierce et al., 2006).

~~As~~ The OHC increase, being a major concern ~~in~~ for both ~~the~~ oceanography and climate communities, ~~the OHC~~ has attracted a great deal of attention. Although direct observational records~~are~~ represent the most reliable~~trustworthy~~ data for~~in~~ determining the oceanic thermal state, the ~~fact is that measurements~~available ~~data~~observations are ~~far from~~not dense enough in both the temporal and spatial domains, especially for the deep and abyssal oceans. The ~~sparseness of~~number of observations has greatly improved since the launch of a global array of profiling floats, the Argo, in the 2000s. However, the spatial resolution of the Argo program ~~of~~ (i.e., approximately 300 km) is not high enough to capture mesoscale structures (Sasaki et al., 2020, hereafter **S2020**). ~~Several~~ There are several approaches ~~exist to~~ for filling the temporal and spatial gaps in global temperature measurements~~,~~ ,~~and~~ which can be used to produce gridded temperature ~~fields~~ products ~~to~~ for ~~estimate~~ estimating the OHC. ~~These~~ Typical approaches include an ~~the~~ objective analysis (Good et al., 2013) of observational data and an ensemble optimal interpolation with a dynamic ensemble (EnOI-DE (Cheng and Zhu, 2016). ~~ocean reanalysis, the later being a combination of physical ocean models with observationsobservational data.~~ In addition, ocean general circulation models (OGCMs) provide the temperature fields by solving ~~the~~ primitive equations of fluid motion and state. When constrained by observations, a numerical ocean modelling becomes the ocean reanalysis, which geneally lacks dynamical-consistence (the resulting fields satisfy the underlying fluid dynamics and thermodynamics equations), unless the adjoint method was adopted to use information contained in observations. ~~Although OGCMs are dynamically consistent (the resulting fields satisfy the underlying fluid dynamics and thermodynamics equations), some models are not constrained by observations.~~ Although ocean reanalysis has been widely constructed, unconstrained OGCMs are still an important tool for climate prediction, for instance, the Coupled Model Intercomparison Project (CMIP). How multi-scale dynamical processes are represented in these unconstrained models and their implementation of external forcing significantly impact their OHC estimates.

The Ocean General Circulation Model for the Earth Simulator (OFES~~;~~ (Masumoto et al., 2004; Sasaki et al., 2004)), developed by the Japan Agency for Marine-Earth Science and Technology (JAMSTEC) and other institutes, is a well-known eddy-resolving OGCM~~ocean model~~, and the hindcast simulation of the OFES Version 1 (OFES1) has been widely used (Chen et al., 2013; Dong et al., 2011; Du et al., 2005; ~~Sasaki et al., 2020;~~ Wang et al., 2013). The hindcast simulation based on the OFES Version 2 (OFES2) has now been released~~, and~~ with certain improvements ~~have been demonstrated~~ over the OFES1 (**S2020**). For example, in a comparsion to the OFES1, the authors found a smaller bias in the global sea surface temperature (SST), sea surface salinity (SSS), and the ~~water~~ water-mass properties~~in~~ of the

Indonesian and Arabian Seasseas in the OFES2. To our knowledge, however, a comparison of the multi-decadal OHC at a basin or global scale from based on data obtained frombetween the OFES1 and OFES2 is lacking. As this high-resolution quasi-global model hindcast simulation is expected to be widely used in the oceanography and climate communities for examining the state of the ocean state in the near future, it is necessary to compare the estimates of OHC estimatesd from determined using these two OFES as an indicator of the potential improvements in the OFES2 over the OFES1,. Such a study is also expected to provide insights on and also of their adaptability of the two simulations forto the OHC-related studies. This is further motivated by the The finding that subsurface oceanic fields could be notably different between when estimated based on the results of two OFES runs with different atmospheric forcing, despite their similar results in the near-surface may be similarregion (Kutsuwada et al., 2019), forms an added motivation to conduct the envisioned study.

—The aim of this studypaper is twofold: (1) to estimate the OHC in the global ocean and in each major basin using the OFES1 and OFES2, with a primary focus on to evaluate their any differences associated withbetween the two hindcasts; and (2) to understand the causes of the differences estimated between based onbetween these two hindcasts. To this end, we used the potential temperature θ to calculate and compare the OHC from 1960 to 2016 for both the global ocean and the major basins, i.e., the Pacific Ocean, the Atlantic Ocean, and the Indian Ocean, between 64° S and 64° N.

—In Section 2, we providegive a brief description ofto the data and methods used in this study here. In Section 3, we describe and discuss the OHC differences in OHC between thein both the temporal and spatial domains. A tentative analysis of the possible causes of thesethe differences waswasis also conducted. SectionSections 4 summarizessummarises the principal points and the possible extensions involving factors that were not examined here due to data unavailability, but although such factors could be important. ThereforeAccordingly, we have added the futureFuture scope of this study work is therefore expected to improve on ourthe associated work here.

2 Data and Methods

2.1 Data

The potentialPotential temperature θ from both the OFES1 and OFES2 were used to calculate the global and basin OHCs. This allowed us to compare the results on OHC obtainedestimated from OFES1 and OFES2 for comparison with each other ,and along with the OHC calculatedestimates from the observation-based EN4. Although results from the EN4 cannot be consideredtaken as to represent the actual oceanic state, it has been widely used in OHC-related studies (Allison et al., 2019; Carton et al., 2019; Häkkinen et al., 2016; Trenberth et al., 2016; Wang et al., 2018). A brief description of the three datasets is given below; readers are referred to Sasaki et al. (2004), Sasaki et al. (2020), and Good et al. (2013) for a more detailsdetailed description.

—The OFES1 has a horizontal spatial resolution of 0.1° and with 54 vertical levels with and a maximum depth of 6065 m (Sasaki et al., 2004).; this Such a high lateral resolution enables it to resolve mesoscale processes. Following a 50-year climatological simulation, the hindcast simulation of the OFES1 was integrated forward, with the publicly available data from 1950 to two years ago (the publiclypublically available data is untiltill 2017). The multi-decadal integration ~~period~~ ~~makes~~ made it possible to ~~perform an analysis of~~analyze oceanic fields at temporal scales from intra-seasonal to multi-decadal. Unlike most other datasets used for the estimation of the OHC ~~estimates~~, ~~the~~ OFES1 is an ocean model~~modelling~~ with no observational constraints. Therefore, it can be used to demonstrate ~~the potential benefits of high resolution and~~ the adaptability of high-resolution numerical mode~~l~~ling without data assimilation in climate studies.

~~—The~~ OFES2 has the same horizontal spatial resolution of 0.1°. Vertically, there are 105 levels~~,~~ with a maximum depth of 7500 m. ~~The~~ OFES1 uses ~~daily~~ National Centers for Environmental Prediction (NCEP) reanalysis (2.5° × 2.5°; Kalnay et al., 1996) for ~~the~~ atmospheric forcing on an everyday basis, whereas ~~the~~ OFES2 ~~is forced by~~obtains atmospheric forcing from the ~~3-hourly atmospheric surface dataset~~ JRA55-do Version 08 (55 km × 55 km; Tsujino et al., 2018) ~~.~~with a temporal resolution of 3 h. Both the temporal and spatial resolutions of ~~the~~ atmospheric forcing have increased ~~greatly~~ significantly in the OFES2. The OFES2 also incorporates river runoff and sea-ice models, but ~~no inclusion of~~ polar areas are not included.

~~—~~In the horizontal direction, both ~~the~~ OFES1 and OFES2 use a biharmonic mixing scheme to suppress the computational noise (**S2020**). The horizontal diffusivity coefficient is equal to -9×10^{9} m^{4}/s at the ~~Equator~~ equator (**S2020**)~~,~~ and varies proportionally~~proportional~~ ~~to~~ with the cube of the cosine of the latitude (personal communication with Hide Sasaki) ~~and~~. The OFES2 uses a mixed-~~-~~layer vertical mixing scheme (Noh and Jin Kim 1999) with parametrization of tidal energy~~tidal-energy~~ dissipation (Jayne and St. Laurent 2001; St. Laurent et al., 2002), whereas ~~the~~ OFES1 uses the K-profile parameterization (KPP) scheme (Large et al., 1994). ~~With~~ Taking the temperature and salinity ~~on~~ of ~~1st~~ January 1, 1958~~,~~ from ~~the~~ OFES1 as the initial conditions, ~~the~~ OFES2 ~~used here~~ was~~has been~~ integrated forward, with the publicaly available data from 1958 to 2016. To reduce the computation time ~~and the archive cost~~, we subsampled the OFES1 and OFES2 data at every five~~5~~ grid points in the horizontal direction.

~~—~~To evaluate the OHC ~~objectively~~ from the two OFES data, we used ~~the~~ EN4 from the UK Meteorological Office Hadley Centre as a reference. Note that ~~the~~ we used the EN4.2.1 as the EN4 version ~~we used~~ was~~is the EN4.2.1~~, with ~~bias~~ bias-corrected following Levitus et al. (2009). The EN4 data can be considered as ~~an~~ objective analysis data that is ~~primarily~~ based on observations (Good et al., 2013), with a horizontal resolution of 1° and 42 vertical levels down to 5350 m. The EN4 assimilates data ~~mainly~~ mostly from the World Ocean Database (WOD) and the Coriolis dataset for ReAnalysis (CORA). Pre~~–~~processing and quality checks were~~are~~ conducted before the observational data were~~are~~ used to construct this objective analysis product.

~~—~~Although we used the results from EN4 ~~results~~ as a reference for evaluating the performance of OFES ~~performance~~ in simulating the 57-year thermal state of the ocean ~~thermal state~~, ~~the~~ EN4 cannot be ~~taken~~ considered ~~as~~ to represent the actual ocean state. The main reason is that the measurements used to construct the EN4 datasets are sparse and inhomogeneous in both ~~the~~ temporal and spatial domains, and are ~~far from~~ insufficient to resolve mesoscale or even sub–mesoscale motions. There are ~~are more~~ more observations in the ~~Northern~~ northern ~~Hemisphere~~ hemisphere than compared to the ~~in the Southern~~ southern hemisphere~~Hemisphere~~, and there is also a seasonal bias in the observational data density (Abraham et al. 2013; Smith et al. 2015). A ~~higher~~ larger density of data ~~became~~ was generated~~available~~ only after the World Ocean Circulation Experiment (WOCE) was conducted in the 1990s and following the launch of the Argo profiling floats in the 2000s. Table 1 summarizes the~~these~~ three ~~ocean~~ datasets.

Table 1. ~~Description~~ A summary of the OFES1, OFES2 and EN4 ~~datasets~~. The symbol / means "not applicable".

	OFES1	**OFES2**	**EN4**
Model	MOM3	MOM3	/
Horizontal coverage	75° S – 75° N	76° S – 76° N	83° S – 89° N
Grids	3600 × 1500	3600 × 1520	360 × 173
Vertical levels	54	105	42
Maximum depth	6065 m	7500 m	5350 m
~~Vertical levels~~	~~54~~	~~105~~	~~42~~
Atmospheric forcing	Daily NCEP/ NCAR reanalysis	3–hourly JRA55–do Ver.08	/
Data assimilated	/	/	WOD, CORA
Time span	1950 – 2017	1958 – 2016	1900 – 2021

—We considered water from the sea surface to ~~around~~ approximately 2000 m, and divided it into three layers: upper (0–300 m),~~;~~ middle (300–700 m),~~;~~ and lower (700–2000 m). The ocean above 2000 m ~~has~~ is often ~~been~~ divided into two layers, 0–700 m and 700–2000 m (or even one: 0–2000 m) (Allison et al., 2019; Hä~~a~~kkinen et al., 2016; Häkkinen et al., 2015; Levitus et al., 2012; Zanna et al., 2019~~);~~). ~~our~~ However, our analysis ~~here~~ shows~~will show~~ that it is ~~in fact~~ necessary to divide it into three layers ~~for our purpose~~to reach the objective of this study. Similar vertical division can also be seen ~~did~~ in Liang et al. (2021).

–The reasons for ignoring water below 2000 m were~~are~~ mainly fourfold. First~~Firstly~~, the simulated behavior~~behaviour~~ of the deep ocean depends ~~sensitively~~ on the spin-up of the numerical simulation, which is mostly ~~almost always~~ incomplete (Wunsch 2011), at least in the first decade. Second~~Secondly~~, the observational data used in ~~the~~ EN4 are largely confined to the ~~ocean above~~top 2000 m~~(~~, and ~~many~~ some available measurements do not even go down to this de~~ep~~pth (personal communication with the EN4 UK Meteorological Office Hadley Centre)~~), with a~~. ~~much lower~~The ~~density~~ number of data is significantly lesser in the deep and abyssal oceans. Third~~Thirdly~~, the EN4 data ~~in the EN4 version~~ that we used here ~~are~~ was bias~~-~~-corrected~~,~~ following Levitus et al. (2009), in which only the ocean above 700 m was considered. ~~Therefore, for~~ For instance, the Expendable Bathythermograph (XBT) profiles below 700 m were~~are~~ corrected using the correction values provided for 700 m (personal communication from the UK Meteorology Office Hadley Centre). ~~Finally~~Finally,~~Lastly,~~ ~~as can be seen,~~ the maximum depth of OFES2 and EN4 differs by more than 2000 m ~~between the OFES2 and EN4~~. It was found~~fe~~evinced~~It~~ that ~~a~~ the full-depth OHC, ~~is not highly comparable between~~ estimated using the three datasets, is not highly comparable. ~~This,~~ However~~however~~, this does not imply that we can ignore the contribution of the deep ocean ~~can be ignored~~; it can play an essential role in regulating the global-ocean thermal state (Desbruyè~~e~~res et al. 2016; Desbruyères et al. 2017; Palmer et al. 2011). It is expected that a ~~much~~ significantly better understanding of the deep and abyssal ocean states~~state~~ will be gained with the implementation of the Deep Argo program, which is partially validated by Johnson et al. (2019).

2.2 Methods

We compared the three datasets for~~over~~ the period 1960–2016. In this paper, the OHC represent the OHC anomalies relative to the OHC estimates of~~in~~ 1960. At each grid point, the OHC is ~~given~~ expressed as follows~~by~~:

$$\text{OHC} = \rho \delta v C_p (\theta - \theta_{1960}) = \rho \delta v C_p \Delta\theta, \quad (1)$$

where ρ is the seawater density (kg/m^3),- δv is the grid volume (m^3), C_p is the specific heat of seawater at constant pressure (J/kg/°C), θ -is the yearly potential temperature (°C), and θ_{1960} -is the averageaveraged potential temperature in during 1960. The total OHC in the upper ocean layer (above 300 m) is the integral of Eq. (1) from 0 to 300 m. Similar procedures were appliedapply to the other two layers (300–700 m and 700–2000 m). A value of 4.1×10^6 kg -J/m^3/°C was used for the product of ρ and the specific heat of seawater C_p (Palmer et al., 2011).

—OHCs Both of both the global and individual basinsindividual basin OHCs were calculated for comparison. Fig. 1 shows the domains of the Pacific, Atlantic, and Indian Oceans between 64° S and 64° N, with including their respective marginal seas included. The Our definition of the marginal seas of each major basin may be inconsistent with thosesome of other studies. The major water passages connecting the different basins are showndenoted by red lines also labelled in Fig. 1a. Fig. 1b is A schematic diagram shows the schematic of primary processes that determinedetermining the OHC of an ocean basin (Fig. 1b).

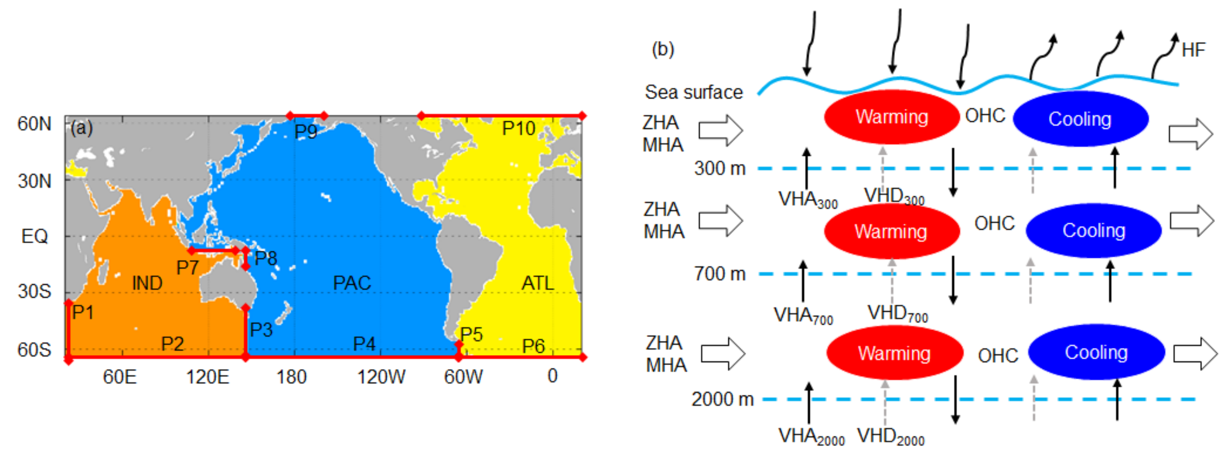

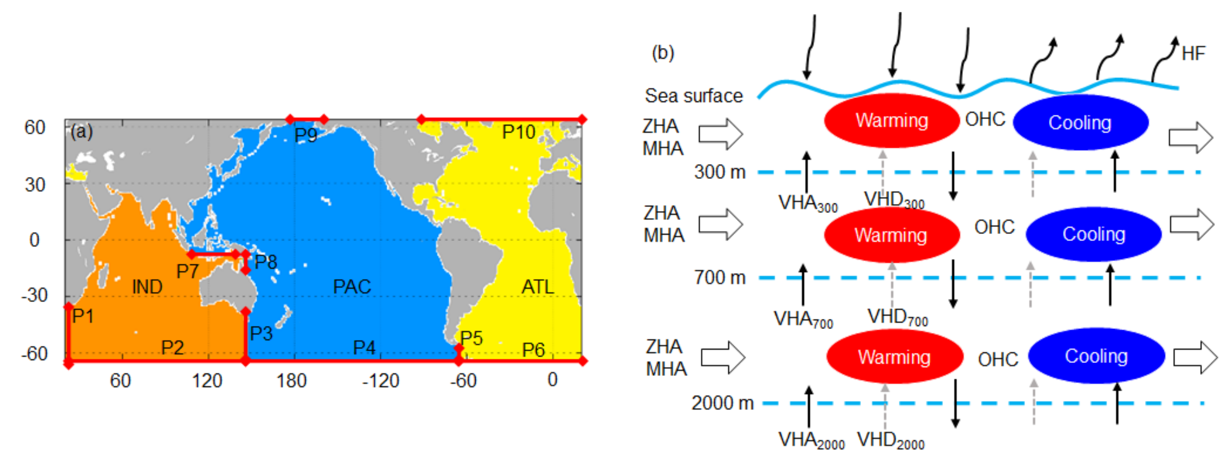

Figure 1. (Left) Domains of the major basins between 64° S and 64° N and (right) a schematic diagram of the primary processes controlling the thermal state of an ocean. (**a**) The PAC stands for the Pacific Ocean, the ATL for the Atlantic Ocean and the IND for the Indian Ocean. The basin domain is extracted using the gcmfaces package (Forget et al., 2015) and then interpolated to the corresponding grid of each product. Grey indicates the land. The red solid lines with diamond arrow stand for the water passages connecting different basins. We label it with the capital letter P (abbreviation for passage) and a serial number. The horizontal and vertical axis are longitude and latitude, respectively.EQ stands for the Equator. (**b**) We use a light blue solid curve to represent the free sea surface and three dashed lines to indicate the 300 m, 700 m and 2000 m depth. The curve arrow represents the net heat flux (HF) through

the ocean surface. The black hollow arrows show the zonal (ZHA) or meridional (MHA) heat advection. The black thin arrow represents the vertical heat advection (VHA) and the grey dash arrow stands for the vertical heat diffusion (VHD). The red ellipse illustrates warming water and the blue ellipse cooling water. P1: (20° E, 64° S – 34.5° S); P2: (20° E – 146.5° E, 64° S); P3: (147° E, 64° S – 36.5° S); P4: (147° E – 65.5° W, 64° S); P5: (67° W, 64° S –55° S); P6: (65° W – 19.5° E, 64° S); P7: (118.5° E – 138.5° E, 8.5° S); P8: (142° E, 12.5° S – 8° S); P9: (172.5° W – 166.5° W, 64° N); P10: (88° W – 19.5° E, 64° N).

—In addition, ~~the~~ Δθ at a fixed depth is~~are~~ decomposed into a heave (HV) component (the second term ~~in~~ of Eq. (2) ~~below~~) and a spice (SP) component (the third term ~~in~~ of Eq. (2)) (Bindoff &~~and~~ McDougall, 1994). ~~The~~ HV-related warming or cooling is manifested as~~a result of~~ ~~the~~ a vertical displacement of the neutral density surfaces (a continuous analog~~analogue~~ of discretely referenced potential density surfaces~~;~~ (Jackett and McDougall, 1997)). In general, both the dynamic~~dynamical~~ changes and the change in the renewal rates of ~~water~~ water-masses can induce vertical displacement, ~~and thus~~generating ~~the~~ HV-related warming or cooling ~~as a consequence~~ (Bindoff and McDougall, 1994). ~~The~~ SP represents warming or cooling as a result of density compensation in ~~the~~ θ and salinity (S) along the neutral density surfaces. ~~This d~~Decomposition of Δθ helps to better understand the contributions ~~and ways~~ of different water~~-~~-masses ~~in~~ to ~~accounting for the~~generating OHC. The formula for decomposing the potential temperature is given as follows:

$$\left. d\theta/dt \right|_z = -\overbrace{\left. dz/dt \right|_n d\theta/dz}^{\mathrm{HV}} + \overbrace{\left. d\theta/dt \right|_n}^{\mathrm{SP}} \quad , \qquad (2)$$

where t is the time (year), z is~~means~~ the depth (m), and $|_n$ means along the neutral density surface.

~~—A~~ The program developed by Jackett and McDougall (1997) was used to calculate the neutral densities, HV, and SP. This code is based on ~~the UNESCO (the~~~~The~~ United Nations Educational, Scientific and Cultural Organization (UNESCO), 1983 for the computation of fundamental properties of seawater (http://www.teos–10.org/preteos10_software/neutral_density.html~~);~~). ~~we~~ We used its MATLAB~~Matlab~~ version for our calculations. The main inputs for this program were~~are~~ ~~the~~ θ and S. ~~As~~ The the code limits the latitude to between 80° S and 64° N, but we further confined our investigation domain to ~~be~~ 64° from the equator,~~;~~ which~~this~~ ~~also~~ avoids comparisons in sea-ice-impacted~~sea-ice impacted~~ areas, ~~knowing~~ given that only ~~the~~ OFES2 includes a sea-ice model.

—To analyze the ~~causes~~ origin of the differences in OHC ~~differences~~ from thermodynamic and dynamic perspectives, we calculated the surface heat flux (HF), zonal heat advection (ZHA), meridional heat advection (MHA), and vertical heat advection (VHA). Owing to a temporary suspension of the OFES2 data by the JAMSTEC, we could not access the vertical diffusivity data of ~~the~~ OFES2 ~~(OFES1 does not provide these data) when~~ while preparing this manuscript. Note that OFES1 does not provide such data. This ~~prevents~~ prevented us ~~to~~ from directly ~~comparing~~ comparing the estimates of vertical diffusion of heat ~~from~~ based on ~~the~~ OFES1 and OFES2. Alternatively, we calculated the residual of the total OHC and all the other heat inputs (HF, ZHA, MHA, and VHA), and used~~took~~ ~~this~~ the results as a proxy for ~~the~~ vertical diffusion. As the horizontal heat diffusion was found to be ~~much~~ significantly weaker than that~~the~~ of ZHA and MHA (not shown), we did not include it in the analysis. A ~~diagram~~ schematic of the primary process~~processes~~ is shown in Fig. 1b. Note that the linear trend in the following sections was calculated using ~~the~~ multiple linear regression using least squares~~, and we used the~~ at 95% confidence level.

3 Results

The principal ~~aim here~~objective of this study is to compare the results from ~~the~~ OFES1 and OFES2,~~, with~~ considering ~~the~~ EN4 ~~acting as~~ an observation-based reference. ~~If~~ We attempted to evaluate if there ~~was a~~is any significant difference between the results obtained from OFES2 ~~result~~ and ~~that~~ those ~~of~~ from one or both of the other two datasets, and ~~does this~~if any such difference represents a real phenomenon that is not present in the other two widely used datasets~~,~~ or ~~is~~ it is an unwanted property of the newly released OFES2 simulation~~?~~. In this section, we compare the three sets of results for the global ocean, ~~and for each~~along with individual cases of the Pacific, Atlantic, and Indian Oceans ~~individually~~.

3.1 ~~Time~~ Temporal evolution of the OHC, HV, and SP from 1960 to 2016

3.1.1 ~~The t~~Time series of OHC, HV, and SP

Fig~~s.~~ures 2–4 ~~present~~ illustrate the time series of the total OHC, and its HV and SP components for the upper (0–300 m), middle (300–700 m), and lower (700–2000 m) ocean layer, respectively. Note that OHC, HV, and SP were calculated as ~~the~~ an anomaly relative to the estimates in 1960, ~~and~~ which was converted to an equivalent HF~~heat flux~~ applying over the entire surface area of the Earth.

Upper layer

For the ~~the~~ global ocean between 0 and –300 m, all three data indicate cooling from ~~around~~ approximately 1963 to 1966 (Fig. 2a), which ~~is~~~~has been explained~~was caused by the ~~as the result of the~~ volcanic eruption of Mount Agung (Balmaseda et al., 2013). A similar trend of cooling ~~over~~ during this period ~~can also be seen~~is also reported ~~in Domingues et al. (2008) and Allison et al. (2019)~~ for the upper 700 m ~~in~~ (Domingues et al.~~ (~~, 2008~~) and~~; Allison et al., ~~(~~2019) ~~(their Fig. 1)~~ and ~~Achutarao et al. (2007) for~~ for both ~~the~~ 0–700 m and 0–3000 m depth (Achutarao et al., 2007)~~(their Fig. 1)~~. This short, ~~but~~ however, sharp cooling period ~~was found to~~ significantly ~~mainly~~ impacted the Pacific Ocean (Fig. 2b). Marked ~~OHC~~ reductions in the OHC associated with ~~the~~ strong volcanic eruptions of El Chichón in 1982 (a strong El Niño ~~ENSO~~ also emerged in 1982–83)~~,~~ and Pinatubo in 1991 were also consistently captured by all ~~the~~ three data.

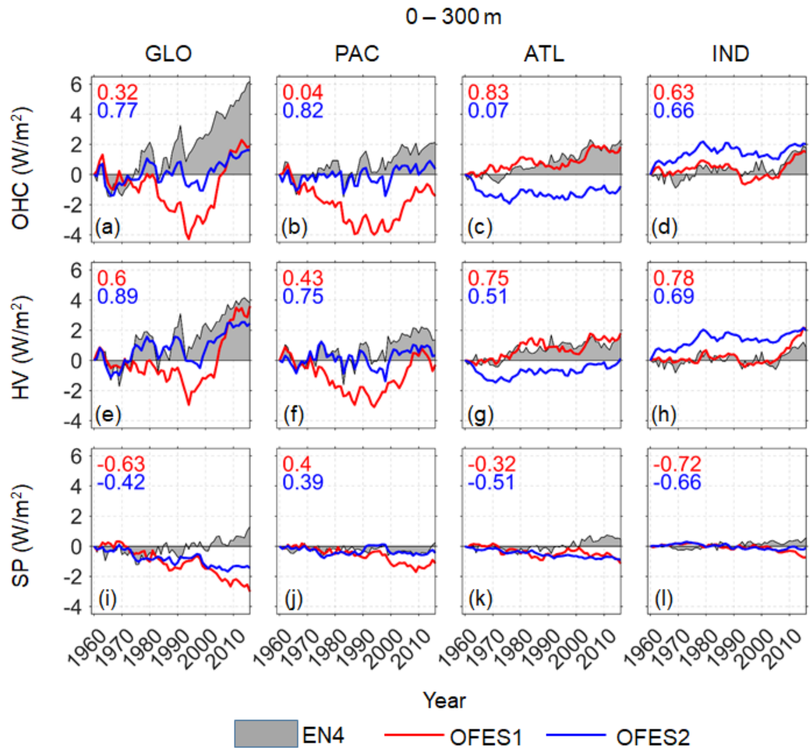

Figure 2. Time series of the global and basin–wide OHC (**top**), HV (**middle**) and SP (**bottom**) between 0–300 m based on the three temperature productsdatasets. The OHC, HV and SP here are converted to the accumulative heating in W/m^2 applied over the entire surface of Earth. Grey shadow: EN4; red solid line: OFES1; blue solid line: OFES2. Numbers on the left top corners are the correlation coefficients between the OFES1 (red) or OFES2 (blue) and EN4. The OHC hereafter is directly calculated from the potential temperature, rather than the sum of the HV and SP.

—Both the EN4 and OFES2, but not the OFES1, showed a slowdown in warming and even cooling in the Pacific Ocean during the 2000s (Fig. 2b). This slowdown of warming in the Pacific warming corresponded corresponds to to a sharp warming trend in the upper layer of the Indian Ocean (Fig. 3d), seen in all the three datasets. This relationshiprelevance between the Pacific and Indian Oceans was found to becould be a consequence of an intensifyingintensified Indonesian ThroughflowThroughflow, leading towhich an increased heat transport from the Pacific to the Indian OOceans (Lee et al. 2015; Zhang et al. 2018);). Note thathowever, these two studiesreferences considered the top 700 m. As will be shown, Howeverhowever, this the sudden warming of the Indian Ocean was largely confined to the the oceanic region abovetop 300 m, especially which is as indicated by the OFES1 and OFES2 (Fig. 3d). The EN4 showed a clear acceleration of warming trend above 300 m acceleration around 2003 in the global ocean above 300 mduringaround 2003, which was probably an artifactartefact of the transition of the ocean observation network from a ship-based system to Argo floats (Cheng and Zhu, 2014), although these authors mainly used subsurface temperature data from the World Ocean Database 2009 (WOD09). Interestingly, a dramatic shift can also be seen in the OFES1 (Fig. 2a), indicatingrememberingalthough that the OFES1 is not directly constrained by observations. A major difference in this jump between the EN4 and OFES1 is that it was found to be more its closely associated association with the SP in the EN4 (Fig. 2i) but with thecompared to HV in the OFES1 (Fig. 2e). This spiciness warming around 2003, derived from objective analysis of observational data, ~~can serve as a~~ complements to~~of~~ the work of~~by~~ Cheng and Zhu (2014).

~~—~~However, ~~many~~ several significant differences were~~can be~~ ~~found~~ observed between the three datasets. ~~The~~ Results from EN4 indicated that ~~an approximately linear~~ the temporal evolution of the warming was approximately linear since ~~around~~ ~1970 (Fig. 2a), which was modulated by the abovementioned climate signals. The OFES1, however, showed that the cooling period persisted almost until the ~~beginning of the~~early 1990s, ~~when~~ while a similar linear but stronger warming trend appeared afterward~~s~~ (Fig. 2a~~);~~). ~~this~~ This was more than 20 years later than that indicated by the EN4. In the OFES2, ~~The~~ the approximately linear warming trend appeared even later ~~in the OFES2 from around~~~~during~~(~2000), ~~and~~ the magnitude of which was approximately the weakest among the three datasets.

~~—~~Compared to ~~the~~ OFES1, the temporal profile of the global upper ocean obtained using OFES2 agreed better with ~~the~~ that indicated by EN4 ~~in the temporal profile of the global ocean~~ (Fig. 2a), which, to some extent, is consistent with the smaller SST~~sea surface temperature (SST)~~ bias estimated from the OFES2 than that from the OFES1 when compared~~comparing~~ to the World Ocean Atlas 2013 (WOA13) (**S2020**). However, the~~re~~ difference between OFES2 and EN4 in magnitude ~~was a~~ became larger ~~magnitude difference~~ after 1980. This was~~came~~ mainly due to~~from~~ the ~~spiciness~~ SP component (Fig. 2i), with both ~~the~~ OFES1 and OFES2 indicating a clear SP cooling episode. This ~~may~~ might imply some discrepancies in the salinity characteristics of~~from~~ these three datasets~~data~~. In contrast, there was ~~quite~~ good agreement between~~in~~ the HV values of~~from~~ ~~the~~ EN4 and OFES2 (Fig. 2e).

~~—~~Clear differences can also be ~~easily discerned~~seen for each ~~individual~~ basin. The OFES1 differed significantly from the other two in the Pacific Ocean ~~between around~~during -1970–1990, with the other two being similar to each other ~~in~~ with respect to both ~~the~~ HV and SP. In the Atlantic Ocean, however, the OFES1 agreed quite well with the EN4 ~~quite well~~ in the HV. Although the two OFES datasets had similar spiciness in the Atlantic Ocean, they both disagreed with the spiciness of~~from~~ ~~the~~ EN4. The HV, ~~indicated by~~estimated using ~~the~~ OFES2, showed poor agreement with both ~~the~~ EN4 and OFES1 in the 1960s (Fig. 2g). In the Indian Ocean, ~~the~~ OFES1 was much closer to ~~the~~ EN4 than to~~the~~ OFES2. Both the similarities and differences in the OHC ~~came largely~~ were associated mostly with ~~from~~ the HV, which dominant~~ed~~ly influenced~~dominates~~ the variation in~~of~~ OHC. The notable deviations of the OFES2 relative to others ~~mainly come~~were mainly generated from the uniquely strong warming trend in the OFES2 Indian Ocean before ~~around1980~~ ~1980 (Fig. 2d).

~~—~~A potential issue of the OFES2 is the spin-up, although it ~~started~~ was initiated from the calculated ~~the~~ temperature and salinity fields from OFES1. Without ~~a~~ any prior knowledge of~~about~~ ~~when it is fully~~the timing of complete spun-up, here we have ~~here~~ shown and compared ~~its~~ the simulated results ~~starting~~ from 1960, ~~only~~ excluding the first two years (1958–1959). It seems that the results obtained using OFES2 ~~has~~ have a ~~good~~ better agreement with ~~the~~ EN4 since the~~around~~ 1980s for~~in~~ both ~~the~~ Atlantic and Indian Oceans (Fig. 2c, d), which is likely to be related to the ~~the better~~improvement in spun-up with time. However, in the Pacific Ocean, the OFES2 was quite similar to ~~the~~ EN4 before 1990, especially ~~in~~ ~~the~~ its HV component. This~~ observation~~, to some extent, ~~may~~ might weaken the spin-up argument.

Middle layer

In the middle ocean layer (300–700 m) (Fig. 3), there were remarkable differences in the OHC and its HV and SP components between the OFES2 and the other two datasets, which is most noticeable ~~for the global ocean and~~in the Atlantic Ocean, and lesser ~~so~~ for the Pacific Ocean; ~~there was~~the difference was ~~little~~ minor ~~difference~~ for the Indian Ocean. The OFES2 showed a moderate Pacific cooling for almost the entire~~whole~~ 57–year period and a strong Atlantic cooling trend until ~~around~~ ~2000, with a subsequent hiatus in the Atlantic Ocean. The OFES2 indicated that t~~T~~here was a minor ~~Indian~~ cooling in the Indian Ocean ~~from the OFES2 in~~ during the 1960–70s. In ~~the~~ OFES2, ~~this~~ these uniquely cooling trends ~~was~~ were mainly generated due to the decreasing HV~~, as~~ because its spiciness was ~~significantly~~generally ~~largely~~ more positive than the other two.

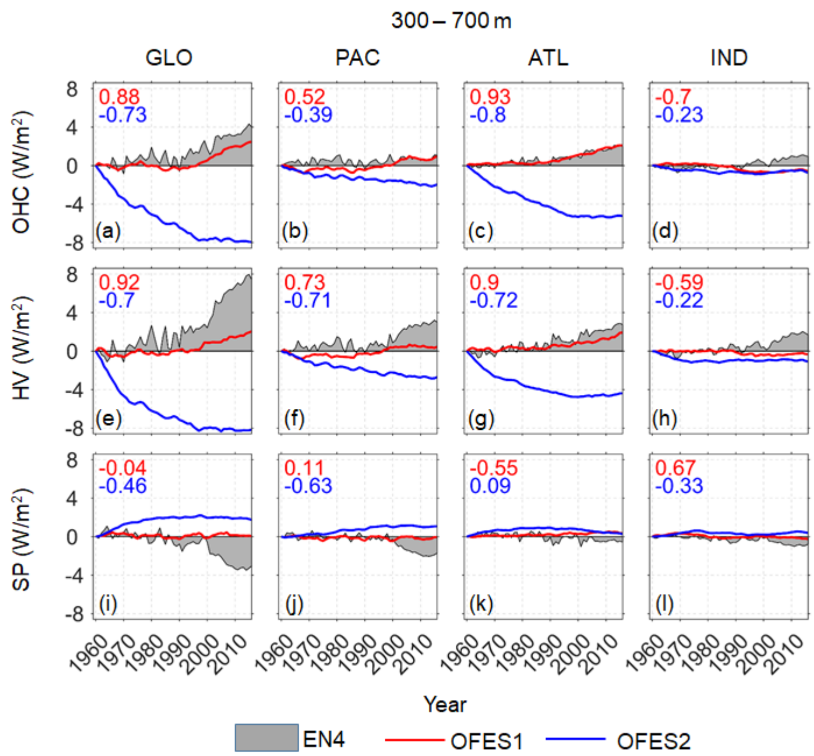

Figure 3. As for Fig.2 but for the middle layer (300–700 m).

—In contrast, both ~~the~~ EN4 and OFES1 indicated that ~~this~~ the middle layer was relatively stable before ~~about~~ the early 1990s. ~~Then, the~~ EN4 and ~~the~~ OFES1 both showed ~~the~~ global ocean and ~~the~~ Atlantic Ocean warming (Fig. 3a, c), mostly due to an increase in the HV (Fig. 3e, g). Despite ~~this~~ such good agreement between ~~the~~ EN4 and OFES1, there were notable differences in their HV and SP components. Compared to the OFES1, there was a ~~generally~~ stronger positive HV in the EN4 (Fig. 3e–h)~~,~~ and a stronger ~~but~~ negative SP in the EN4, particularly after ~~approximately~~about 2000 (Fig. 3i, j). A possible reason for this ~~observation~~finding ~~is the fact that~~may be that ~~there have been~~ many more observations have become available since the ~~WOCE (~~WOCE~~orld Ocean Circulation Experiment (WOCE)~~ was conducted in the late 1990s and from the Argo since the beginning of the 2000s. This ~~may~~ might have led to a systematic trend in the observation-based ~~observational based~~ dataset EN4. Unlike ~~in the~~ EN4 and OFES2, the SP variations in ~~the~~ OFES1 were almost invisible for almost all the basins. In addition, the aforementioned significant warming acceleration from the early 2000s to the 2010s in the Indian Ocean (Fig. 2d) can still be seen in the EN4 (Fig. 3d), ~~but~~ however, this was almost invisible in the two OFES datasets.

~~—~~One major cause of the profound differences between ~~the~~ OFES2 and ~~the~~ EN4 ~~is~~ may be the spin-up issue. Indeed, even after 2000, clear differences ~~remained~~can be observed~~remain~~ in the global ocean. ~~This, Onon the one hand, t~~This is expected because the middle layer takes more time to be ~~well~~ completely spun-~~ up~~ compared to the upper layer~~; on the other hand, it suggests that.~~ Hence, special caution is ~~needed~~ required ~~when~~ while investigating the multi-decadal variations~~,~~ or even decadal variations in the recent two decades based on ~~the~~ OFES2.

Lower layer

In the lower oceanic layer (700–2000 m) (Fig. 4), the OFES2 was ~~clearly~~ again ~~the~~ an outlier ~~of~~ among the three datasets. It showed that the Atlantic and the Indian Oceans experienced cooling from 1960 to the end of the 1990s (Fig. 4c, d), followed by~~then~~ a slight warming episode. The Pacific Ocean, however, showed~~was shown~~ cooling over the entire~~whole~~ 57-year period (Fig. 4b). The better agreement between the results from OFES2 and ~~with the~~ EN4 since the end of the 1990s ~~may~~ might be related to the spin-up issue of the OFES2, at least to some extent.~~-~~ However, the agreement between ~~the~~ EN4 and OFES2 was even better than that in the middle layer (300–700 m), particularly in the Atlantic Ocean. This ~~may~~ might weaken the spin-~~-~~up argument~~, as~~ because it is expected that the middle layer ~~is~~can be~~was~~ more easily spun-~~-~~up than the lower layer.

~~—~~The variations in OHC ~~variations from~~ determined using ~~the~~ OFES1 and ~~the~~ EN4 were similar~~much the same~~ for the global ocean, ~~but~~ however, this ~~was~~ could be ~~a result of the cancelling~~associated with the cancelation of the substantial differences in the Pacific and Atlantic Oceans (Fig. 4b, c), and in the HV and SP (Fig. 4e–l). ~~Specifically~~More specifically, there was a larger ~~OHC~~ increase of OHC in the Pacific Ocean, when estimated using ~~from the~~ OFES1 than ~~the~~ from EN4, ~~but~~ however, the latter showed a larger increase of OHC ~~increase~~ in the Atlantic Ocean. From the perspective of potential temperature decomposition, ~~the~~ EN4 generally showed a stronger ~~HV~~ increase in HV than ~~the~~ OFES1 in the Atlantic and Indian Oceans (Fig. 4g, h), ~~but~~ however, a stronger negative ~~SP~~ or a weaker positive ~~SP~~ increase of SP is also evinced (Fig. 4i–l).

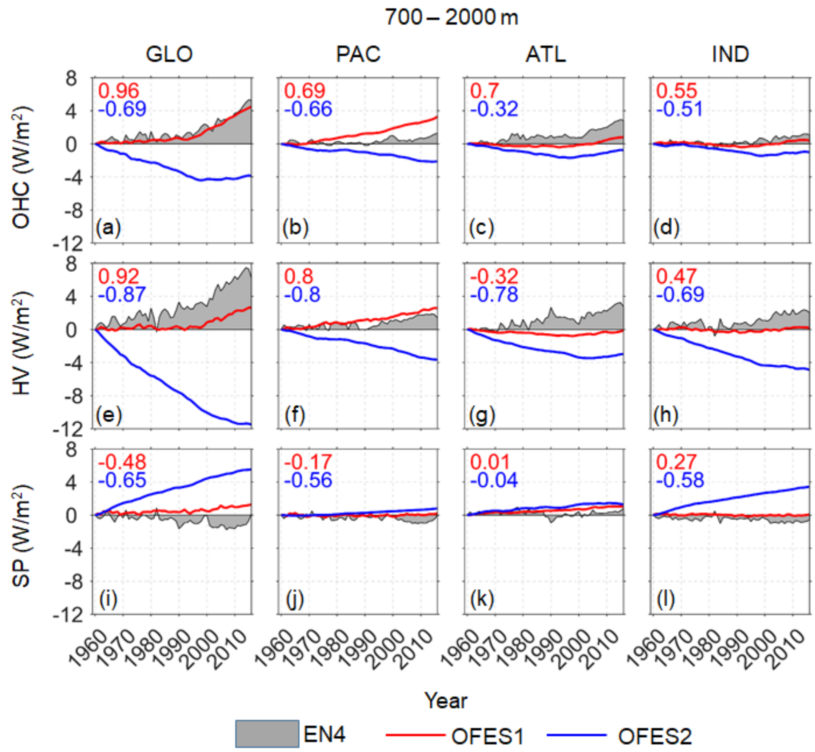

Figure 4. As for Fig.2 but for the lower layer (700–2000 m).

3.1.2 Temporal evolution ~~in~~ of the OHC, HV, and SP trend

Fig~~s.~~ures 2–4 show ~~clearly~~ the similarities and differences between the three datasets ~~in~~ with respect to the time series of ~~the~~ OHC, HV, and SP for the period 1960–2016. In this section, we calculate the linear trend in ~~the~~ OHC, HV, and SP over a rolling window of 10 years for the three datasets~~,~~ following Smith et al. (2015~~);~~), and the results for the three layers are shown in Fig~~s.~~ures 5–7, respectively. ~~This~~ Such evaluation has ~~helps~~ helped us to quantitatively compare the three datasets over each temporal window.

Upper layer

The profile of the 10-year rolling trend of the OHC evaluated based on the three datasets ~~were~~ was similar in shape ~~in the profile of the OHC 10-year rolling trend~~; they captured most of the peaks and troughs pretty ~~well~~consistently. There was a better agreement among the data ~~in~~ for the Indian Ocean (Fig. 5d) ~~than~~ compared to that in the other two basins (Fig. 5b, c), ~~but~~ however, ~~there were still significant~~ notable differences were still observed ~~even~~ in this shallow layer of the Indian Ocean. The rolling trend for the global ocean, estimated from ~~the~~ EN4, was mostly positive ~~most of the time~~, except at the beginning of the 1960s and ~~at~~ the end~~ends~~ of the 1970s and the 1980s (Fig. 5a). However, the OFES1 showed a cooling trend in the global ocean before ~~around~~ ~1990; it then indicated a larger warming trend ~~than~~ compared to that estimated from the other two datasets. The OFES2 generally had a better agreement with ~~the~~ EN4 for the global ocean, ~~but~~ however, the warming trend was ~~much~~ significantly smaller than that estimated ~~from~~ using ~~the~~ EN4 from the late 1960s to ~~around~~ ~1990. Since the beginning of the 1990s, the ~~trend~~ disparity in the trend between ~~the~~ OFES2 and ~~the~~ EN4 was significantly~~much~~ reduced, ~~but~~ ~~however~~although~~,~~ the OFES2 still showed a consistently weaker warming trend. This ~~better~~ improved agreement may be attributed to two factors~~causes~~. First~~Firstly~~, after running the simulation for approximately~~around~~ 30-~~ ~~years~~ running~~, the OFES2 ~~was believed~~is expected to have ~~been~~ developed better spun-up and, therefore, the associated results were closer to the actual state. Second~~Secondly~~, it is also possible that the accuracy of the EN4 data increased as more observational data were included, given that ~~the number of~~ oceanographic observations ~~has~~ have increased significantly since the 1990s (e.g., satellite-based SST measurements and in-situ temperature measurements).

Among the differences observed between the three datasets, the three extreme trend peaks at ~~around~~ approximately 1970, 1980, and 2000 (Fig. 5a) ~~are~~ were particularly prominent, with remarkable differences between ~~the two~~ OFES and EN4, indicating some ~~deficiencies~~ limitations of unconstrained numerical ~~modelling~~models in the reproduction~~reproducing~~ of strong climate events. ~~Apart from some certain minor magnitude differences, the three datasets agreed the best in for the Indian Ocean (Fig. 5d).~~ The OFES1 was closer to ~~the~~ EN4, ~~in~~ showing significant warming in the Indian Ocean in the 2000s, whereas ~~the~~ OFES2 showed a relatively weaker warming trend. ~~A~~ The second better agreement between the three datasets was reached ~~in~~ for the Atlantic Ocean.

It was evinced that ~~The~~ HV has ~~clearly~~ dominated the 10-year rolling trend in all basins (Fig. 5e–h), and the major differences between the three datasets resulted from the differences in the HV component. In addition, there was an ~~apparent~~ general out-of-phase relationship between the HV and SP trends in the global ocean and the Pacific Ocean. This correspondence between the HV and SP is expected for typical stratification in subtropical regions (Hä~~a~~kkinen et al. 2016), with warm and salty water ~~over~~ overlying ~~the~~ cold and fresh water. The OFES1 and OFES2 ~~were~~ provided quite similar~~close~~ results ~~in~~ for the simulation of spiciness, particularly in the individual basins (Fig. 5i–l).

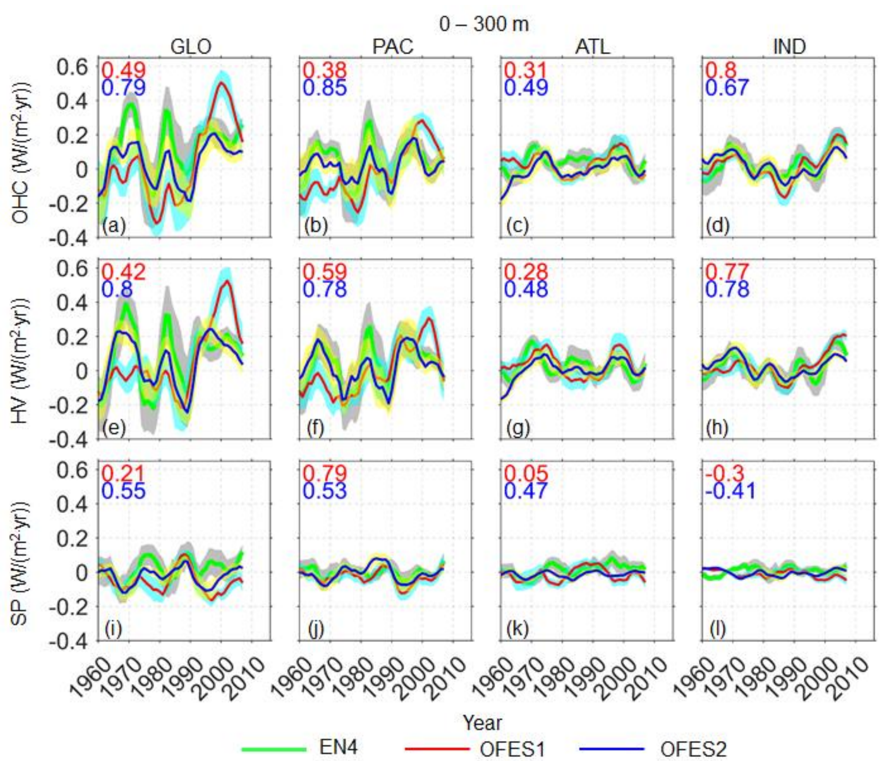

Figure 5. Temporal evolution of the 10-year rolling trends in the global and basin OHCs (**top row**), HV (**middle row**) and SP (**bottom row**) in the top ocean layer (0–300 m), based on the three datasets. Numbers in the top left corners are the correlation coefficients between the EN4 and the OFES1 (red) or OFES2 (blue). The OHC, HV and SP were converted to accumulative heating (W/m^2) over the entire surface of the Earth. Thick green line: EN4 (grey shadow: 95% confidence interval); thin red solid line: OFES1 (cyan shadow: 95% confidence interval); thin blue solid line: OFES2 (yellow shadow: 95% confidence interval).

Middle layer

The variation in the 10-year rolling trend, evaluated ~~from~~ based on ~~the~~ OFES1 and ~~the~~ EN4 datasets, was ~~much~~ found to be mostly ~~the same~~similar for the global (Fig. 6a), Pacific (Fig. 6b), and Atlantic (Fig. 6c) Oceans, ~~but~~ however, the latter dataset had~~having~~ a ~~much~~ significantly larger~~large~~ uncertainty ~~(Fig. 6)~~. The OFES2 showed a significantly different and generally cooling trend, especially concentrated in the Atlantic Ocean, consistent with Fig. 3~~,;~~. The origin of ~~and~~ the ~~reasons why~~ notable cooling trend and its weakening with time estimated from the OFES2 ~~in~~ for the Atlantic Ocean ~~weakened with time~~ needs to~~a further~~ be~~detailed~~ further studied~~ in detail~~~~study~~. ~~It was found that t~~The cooling trend ~~in~~ of the OHC, estimated from ~~the~~ OFES2, ~~came largely~~was mostly generated from the HV. In the Pacific Ocean (Fig. 6b), the OFES2 consistently showed~~show~~ a weak cooling trend, ~~but~~ however, in the middle and late 1960s and after ~~around~~ ~1980, both ~~the~~ EN4 and OFES1 showed a warming trend of similar magnitudes. The results from OFES1 also agreed well with that from the EN4 ~~in~~ for the Atlantic Ocean, i.e., both ~~indicating~~ indicated a weak warming trend for most of the studied period ~~but~~ along with ~~also~~ a sporadic cooling trend. However, ~~these good~~such agreements ~~are~~ could represent the compensation results of the significantly different HV and SP components ~~from~~ of ~~the~~ OFES1 and EN4. For example, the EN4 showed ~~much~~ a significantly stronger HV warming trend than the OFES1 in the Pacific Ocean since the early 1990s, ~~but~~ however, in the meantime, the EN4 also indicated a stronger SP cooling trend. In the Indian Ocean, ~~the~~ EN4 presented a warming trend over much of the 57- year~~ periods~~, whereas the two ~~OFES datasets based on~~ OFES showed weak variations and reversals between warming and cooling episodes.

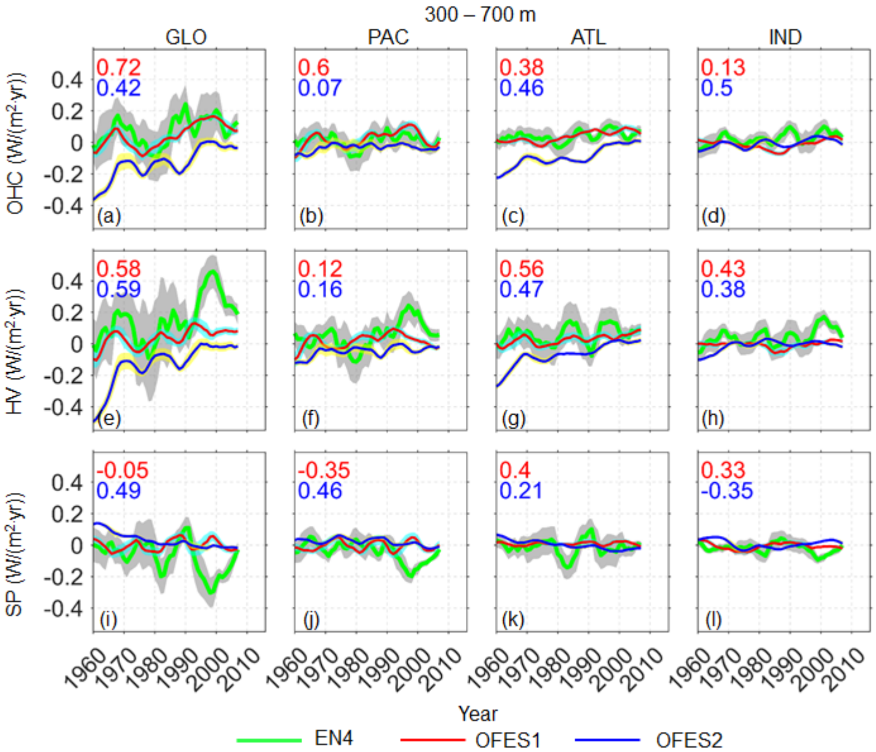

Figure 6. As for Fig. 5 but for middle layer (300–700 m).

Lower layer

As in the middle layer, the OFES2 differed significantly from the other two datasets by ~~showing~~ displaying a cooling trend in the global ocean until approximately~~about~~ 2000 (Fig. 7a). Although OFES2 indicated the appearance of a ~~a~~ warming trend ~~appeared~~ in the global ocean~~ in the OFES2~~after ~2000, the intensity was ~~much~~ significantly lower than that of ~~the~~ EN4 and OFES1. The major differences between the two OFES datasets occurred in the Pacific Ocean (Fig. 7b), and were~~was~~ mostly associated with the HV component~~ associated~~. Despite ~~of~~ the good agreement~~agreements~~ in the OHC trend between the OFES1 and OFES2 ~~in~~ for the Atlantic and Indian Oceans (Fig. 7c, d), their HV and SP components were markedly different, especially in the Indian Ocean (Fig. 7h, l). The OFES1 and ~~the~~ EN4 showed a ~~much the same~~mostly similar global OHC trend (Fig. 7a);~~,~~ ~~but again~~ this was ~~the result of~~ because the significant HV and SP components ~~cancelling~~ canceled each other.

To summarize, the OFES2 ~~showed~~ demonstrated some improvement (better agreement with ~~the~~ EN4) over the OFES1 in the upper layer (above 300 m), but was more of an outlier ~~in the other two layers~~below 300 m. It is essential to examine the HV and SP components ~~when~~ while investigating the OHC trends~~, as~~ because different data products ~~may~~ might show mostly ~~much the same~~similar evolution of the OHC~~ evolution,~~ but substantially different HV and SP.

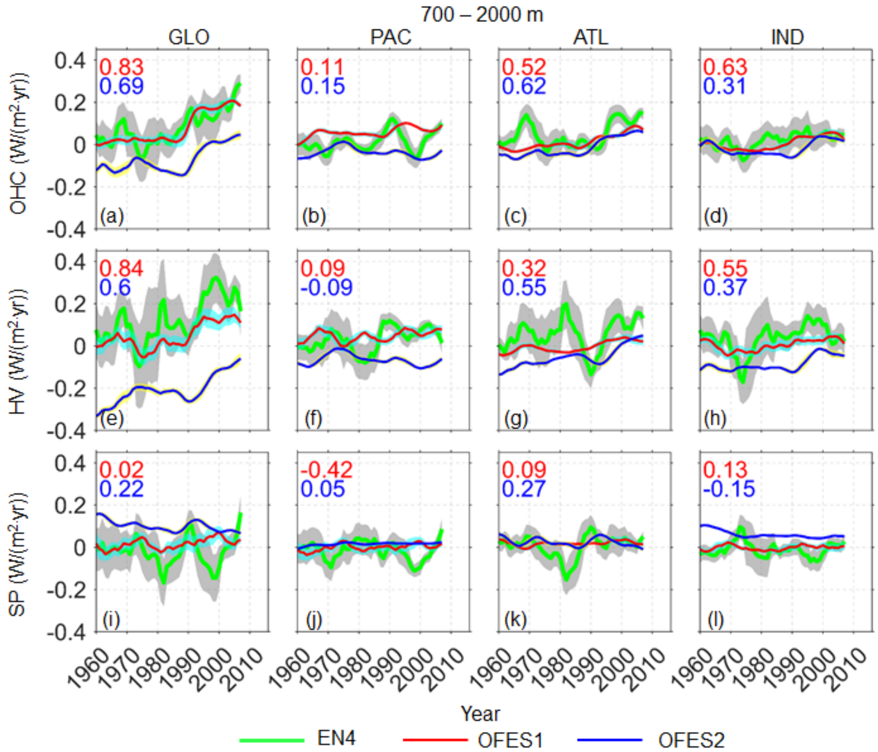

Figure 7. As for Fig. 6 but for the lower layer (700–2000 m).

3.2 Temporal evolution of the zonal-averaged potential temperature trend

Section 3.1 focused on the temporal characteristics of the global and basin-wide OHC, HV, and SP estimated from the three datasets. Although both similarities and differences were demonstrated, ~~this~~ the comparison ~~only~~ in the temporal domain lacked spatial information. In this s~~tudy~~ection~~Here~~, we aimed~~aim~~ to~~at~~ understand~~understanding~~ how the differences were distributed in the meridional direction. As a first step, we calculated the 10-year rolling trends in the zonal-averaged potential temperature ~~change~~ for all three datasets (Figs. 8–10). We also calculated the HV and SP components (Supplementary Information, Figs. 1–6).

—The complex patterns shown in Figures~~.~~ 8–10 defy easy interpretation; therefore, ~~so~~ we have ~~focus~~focused on the large-scale patterns of the observed similarities and differences.

Upper layer

~~There was a generally~~In general, a reasonable ~~correlation~~agreement was observed between ~~these~~ the three datasets at latitudes of 30–60° N for both ~~the~~ Pacific and Atlantic Oceans (there is no northern high latitude in the Indian Ocean). More specifically, ~~there was~~ a wave-like cooling trend propagating from approximately~~around~~ 60° N to 30° N was observed from 1960 to the end of the 1970s in the global ocean; this apparent propagation was especially ~~clear~~ evinced in the ~~the~~ EN4 and OFES2 data. In addition, there was a northward propagation of a cooling trend in the 1990s between ~~around~~ 30 and ~~–~~45° N. It is reasonable to attribute ~~this~~ theses cooling episodes to the volcanic eruptions of Indonesia's

Mount Agung in 1963, Mexico's El Chichón in 1982, and the Philippines' Mount Pinatubo in 1991,~~;~~ and the two hindcast simulations were able to reproduce these climate events.

~~—~~Following these cooling events, there were three subsequent warming trends~~,~~ as the ocean surface temperature returned ~~back~~ to normal ~~once~~ after the aerosols released over several years of volcanic eruptions ~~finally~~ were completely dispersed. Of these warming trends, ~~that~~ the one following the El Chichón eruption was the most significant~~,;~~, and ~~–~~there was a clear northward propagation of ~~the~~ this significant warming trend from ~~around~~ approximately 30° N to the subpolar areas. Interestingly, the contributions of SP to this large-scale warming and cooling episodes ~~by the SP~~ were~~was~~ comparable~~comparably~~ to those of the HV (Supplementary Information, Figs. S1–2), contradicting the general assumption~~sense~~ that ~~the~~ HV ~~dominates~~ is the most dominant contributor of the potential temperature changes. In fact, the abovementioned~~-mentioned~~ propagation of the cooling patch from ~~around~~ approximately 60 °N to 30° N ~~in the~~during 1960–1970~~s~~ was, to a larger~~lager~~ extent, associated with the SP.

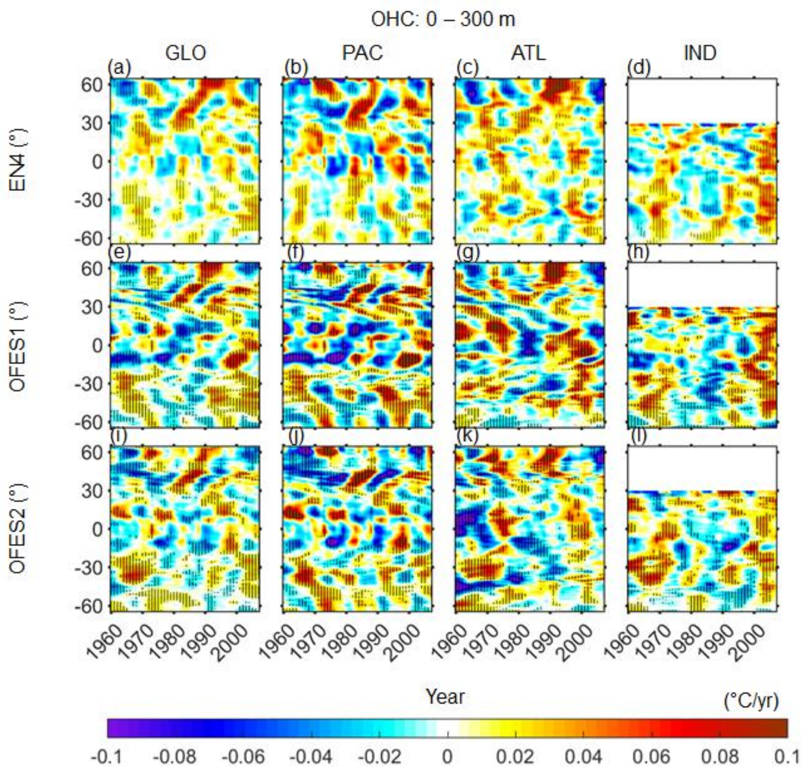

Figure 8. Temporal evolution of 10-year rolling trend of the zonal averaged potential temperature change in the upper layer of the ocean (0–300 m). **Left to right:** global, Pacific, Atlantic and Indian Ocean. **Top to bottom:** EN4, OFES1 and OFES2. Horizontal axis: year; vertical axis: latitude. Stippling indicates the 95% confidence level. The HV and SP counterparts are in the Supplementary Information, Figs. S1–6.

~~—~~Equatorward of 30°, large differences were observed~~emerged~~ ~~in~~ among the three datasets. Strong cooling was particularly visible in the OFES1 in the Pacific tropics before around 1990 (Fig. 8f), corresponding to the persistent cooling ~~in~~ of the global ocean and the Pacific Ocean as estimated ~~from the~~based on OFEES1 in Fig. 2. ~~In t~~The results of OFES2 for the Pacific Ocean~~,~~ indicated clear differences from the EN4 ~~were discerned~~ in the low latitudes before ~~around~~ 1980, and then a ~~similar~~ pattern similar to that~~the~~ of EN4 was simulated by the OFES2. In the Atlantic tropics

(Fig. 8, 3rd column), considerable cooling over 1960s was evinced in the OFES2, which may be ~~a~~ the result of poor spun-up in the OFES2. All three datasets captured the Atlantic tropical warming in the 1970s~~,~~ and from the 1990s to the 2000s, ~~but~~ however, the two OFES datasets estimated~~estimating~~ a ~~much~~ stronger intensity than ~~the~~ EN4, especially the OFES1. In addition, ~~the~~ OFES1 showed ~~a~~ the appearance of significant cooling ~~appearing~~ in the Atlantic tropics during~~in~~ the 1980s (Fig. 8g). Although a similar contemporary cooling was ~~shown~~ demonstrated by the OFES2, its cooling center was shifted several degrees southward. The~~This~~ ~~1980s~~ Atlantic tropical cooling during the 1980s was ~~comparatively~~ significantly weaker in the EN4. Moreover, the OFES2 indicated an approximate 20-year (1960–1980) cooling episode in the vicinity of 45 °S in the Atlantic Ocean (Fig. 8k).~~;~~ ~~this Such a~~A similar cooling trend existed in the 1960s~~ existed~~, ~~but however, the cooling trend revealed by EN4 and OFES1 was weaker in intensity~~but with a relatively weaker intensity in EN4~~, in the EN4 and OFES1~~. In the Indian Ocean, the most significant agreement among the three datasets was observed, ~~which was associated with~~particularly the intense warming in the 2000s. In addition, there were some common cooling patterns observed from the 1980s to the 1990s in all three datasets. Over these latitudes, the HV accounted for more ~~of the~~substantial potential temperature ~~change~~ changes than the SP, with the latter ~~in~~ generally counteracting the HV (Supplementary Information, Figs. S1–2).

—A general property of the similarities and differences between these three datasets is the fact that a better agreement was reached in the poleward of 30° than the latitudes equatorward of 30°. A possible explanation for this latitudinal dependence is that a deeper thermocline at ~~a~~ higher latitudes responded less sensitively to the applied wind stress (Kutsuwada et al., 2019). Kutsuwada et al. (2019) found ~~that~~ certain issues with the NCEP reanalysis wind stress that was used as ~~the~~ atmospheric forcing ~~of the~~in OFES1~~ had some issues, causing a much~~ as it generated a significantly shallower thermocline in the tropical North Pacific Ocean. ~~and t~~Therefore, large negative temperature differences were observed when compared~~comparing~~ to the real observations ~~and~~ along with the data obtained from ~~an~~ OFES version forced by the wind stress from ~~the~~ satellite measurements (QSCAT). The authors also claimed that the ~~JRA~~ JRA-55 wind stress had ~~similar~~ problems similar ~~with the~~to that of the NCEP wind. Indeed, the intense Pacific cooling patches in Fig. 8f were~~was~~ likely ~~to result~~~~be resulting~~generated from the abnormally shallower thermocline in the tropical Pacific Ocean, consistent with Kutsuwada et al. (2019)~~, despite the different~~ although different- temporal periods were considered.

Middle layer

In the ~~middle~~ intermediate layer between 300 and ~~–~~700 m, the three datasets showed relatively poor agreement compared to the upper layer. The OFES2 differed from the others by ~~showing~~ displaying intense cooling before 2000 in the Atlantic Ocean (Fig. 9k) and a moderate but consistent warming trend in the northern Indian Ocean over ~~most of~~almost the entire~~whole~~ period (Fig. 9l). In addition, there were large-scale cooling patches in the northern Pacific Ocean (Fig. 9j) and along the Indian ~~Equator~~ equator (Fig. 9l) from the OFES2, while these cooling patches were not ~~apparent~~ prominent in the other two datasets. These cooling distributions, obtained from OFES2, further ~~show~~demonstrated~~showed~~ ~~where and when~~the place and timing of the cooling trend ~~from the OFES2 in~~ (Fig~~s~~. 3), which ~~occurred and~~ can be at least partially attributed to the spin-up issue of the OFES2. Some similarities between the OFES2 and the other two datasets have emerged in recent decades. For example, similar to EN4 and OFES1, the

OFES2 reproduced the marked warming episodes observed inat the high latitudes of the northern Atlantic Ocean in during the 1980s and the 1990s, and aalong with the subsequent cooling trend (Fig. 9c, g, k), similar to the EN4 and OFES1.

Comparing Upon comparing the OFES1 with the EN4, both similarities and differences can be discerned. The OFES1 generally agreed with the EN4 in regions located at the north to of 30 °N, with some minor a few differences. However, inIn the tropics, however, large differences were found observed between the OFES1 and EN4. For instance, the OFES1 indicated that the northern Indian Ocean was mostly cooling consistently (Fig. 9h), but however, EN4 reflected alternate warming and cooling appeared in the EN4episodes (Fig. 9d). Furthermore, the intense warming and cooling patches in of the southern Atlantic and Indian Oceans , respectively, shown indemonstrated by the OFES1 (Fig. 9g, h), were not clearly visible in the EN4 (Fig. 9c, d). These potential temperature changes mainly resulted from the vertical displacement of the neutral density surfaces, that isi.e., of the HV component (Supplementary Information, Fig. S3). However, the role of the SP cannot be ignored. This was especially clear in the southern hemispheresouthern hemisphere ofin the EN4.

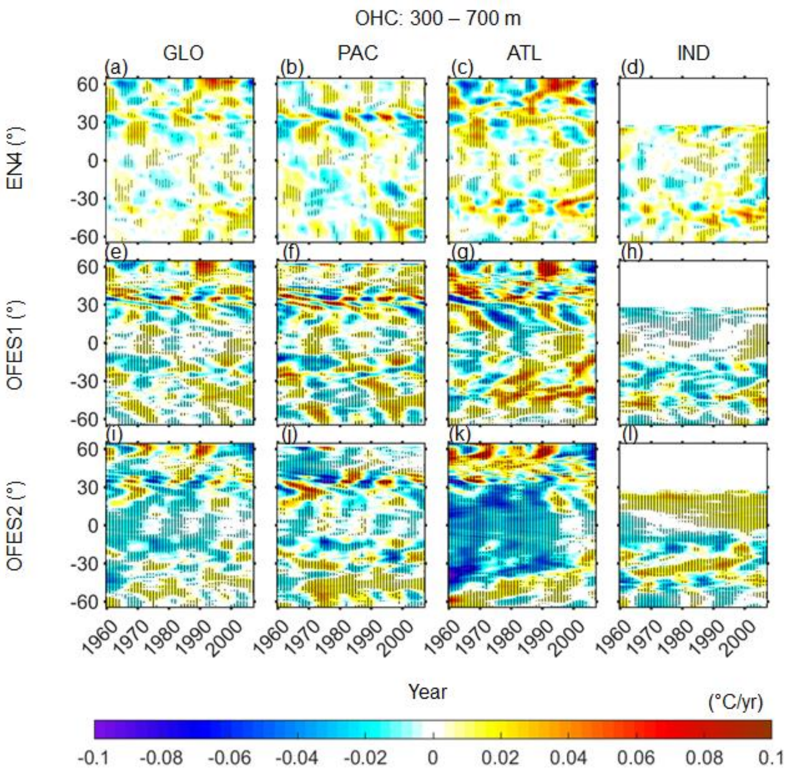

Figure 9. As for Fig. 8 but for the middle layer (300–700 m).

Lower layer

The northern Atlantic Ocean, especially to the nor north ofto 30 °N, dominated the global potential temperature change in the EN4 (Fig. 10). This ; this was mostly related more to the SP, especially in the intense cooling patch (Supplementary Information, Fig. S6). Although the OFES1 data agreed well with the EN4 in the northern Atlantic Ocean (> 30° N), there were considerable differences elsewhere between the OFES1 and EN4. More specifically, OFES1 revealed that there was intense ~~HV associated~~ warming and cooling in the southern Pacific Ocean associated with the HV component ~~in~~ during the 1960s and 1970s ~~in the OFES1~~, ~~but~~ however, such trend was not evinced in ~~the~~ EN4 (Supplementary Information, Fig. S5). In addition, the warming of the southern Pacific Ocean ~~since approximatelyabout 1990~~ was ~~much~~ much stronger in ~~the~~ OFES1 than in ~~the~~ EN4 since approximately 1990~~. The main reason is that there~~, which was associated with the ~~was~~ strong SP cooling in the southern Pacific ~~Ocean~~ Ocean, as revealed in ~~the~~ EN4 (Supplementary Information, Fig. S6). Moreover, OFES1 demonstrated ~~the~~ consistent cooling ~~in~~ of the Atlantic tropics, ~~the~~ significant warming ~~in~~ of the southern Atlantic Ocean, and ~~the~~ intense cooling of the northern Indian Ocean before the middle of the 1990s, which ~~shown by the OFES1,~~ were not evident in the EN4.

The OFES2 data captured some warming patterns in the southern hemisphere~~southern hemisphere~~, similar to the OFES1; it also agreed with the other two datasets in terms of the intense warming patchs in the northern Atlantic Ocean in 1960s and after ~1990. However, the agreement between ~~the~~ OFES2 and the others was generally poor. ~~Most significantly,~~ This was most noticeable in the cooling episode ~~was~~ indicated by the OFES2 at the low and middle latitudes ~~in~~ for both the Pacific and Atlantic Oceans, especially the latter. Furthermore, both ~~the~~ EN4 and OFES2 showed marked but opposite SP variations in the northern Atlantic Ocean to the north of~~to~~ 30 °N, whereas the OFES1 indicated moderate SP in a similar warming/cooling pattern to ~~the~~ EN4.

To summarize, the two OFES datasets had some good agreements with ~~the~~ EN4 ~~in~~ for the upper ocean layer, ~~but~~ however, such general agreement was l~~were l~~argely confined to the middle-high latitudes. ~~Poor~~ In general, the agreement~~agreements~~ was~~were observedfound in the ocean beneath~~for the ocean at lower levels was poor. Specifically, in the middle ocean layer, the OFES1 ~~had~~ displayed a generally reasonable agreement with the EN4 for locations north to 30° N, ~~but~~ however, large differences ~~exist~~ were observed elsewhere~~;~~. ~~in~~ In the OFES2, intensive cooling patches were simulated, especially in the Atlantic Ocean. Although the spin-up issue may partially explain the notable differences between the OFES ~~data~~ and EN4 data for ~~the~~ ocean water below 300 m, other causes ~~responsible for~~might have also contributed toward the examined differences ~~are also possible~~.

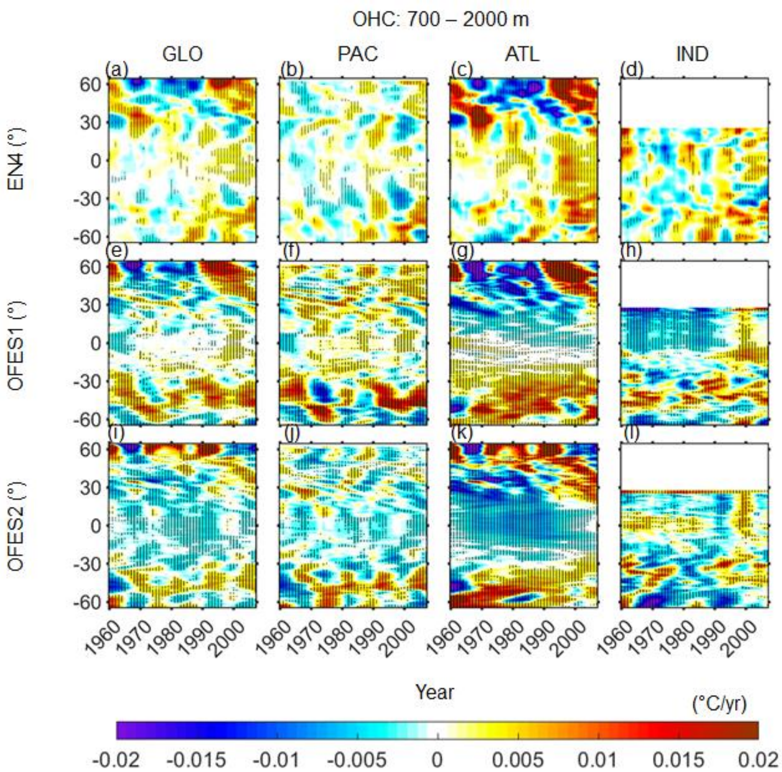

Figure 10. As for Fig. 8 but for the lower layer (700–2000 m). Note the different colour scales.

3.3 Depth-time distribution of potential temperature, HV, and SP trends

—Although we divided the top 2000 m into three layers, some detailsdetail werewas lost in while taking considering the averages of individual layers (i.e., the vertical layers) averages. In this section, we compare the depth-time patterns of the trends in with respect to the changes in potential temperature change ($\Delta\theta_{\mathrm{OHC}}$), and its HV ($\Delta\theta_{\mathrm{HV}}$) and SP ($\Delta\theta_{\mathrm{SP}}$) components (Figs. 11–13).

—For the global ocean, the upper ocean layer above 300 m accounted for most of the warming or cooling trends (Fig. 11, left column). The EN4 showed warming episodes over most of the investigated period, with only a few cooling eventsepisodes as a response to the certain distinctive climate events. It can be seen that the volcanic eruptions of Mount Agung and El Chichón hadimpacted a greater impactdepth than compared to the eruption of Pinatubo. The aforementioned strong cooling episode from the OFES1 in the upper Pacific layer before 1990, which has been estimated from the OFES1, started was initiated at a greater depth in the beginning, and subsequently, endedit terminatedending at a shallower depth (Fig. 11e). At greater depths, moderate warming or cooling trend was observedcan be found. Specifically, in the EN4, moderate warming hascan beenbewas observedseen far deepat larger depths, to at around approximately 2000 m, since around the early 1990s. The OFES1 showed moderate warming between 500 and –1000 m over almost the entirewhole investigated period (Fig. 11e). Since Additionaly, itOFES1 indicated that since around the middle of the 1990s, a weak warming trend has extended to the 2000 m based on the OFES1. The differences inof the results of OFES2 from relative to the other two datasets are apparent in the global ocean below approximatelyaround 200 m, where cooling is the dominant pattern (Fig. 11i); except for some weak warming patches between 500 and –1000 m are exceptions (Fig. 11i).

—In the Pacific Ocean, the OFES2 had a generally reasonable agreement with the EN4 above approximatelyaround 200 m, whereas the agreement between the OFES1 and the EN4 was poorer, despite of some similar warming or cooling patches. Further below, the EN4 showed periodic warming and cooling trends. The OFES1 showed reflected consistent warming between around 500 and –1200 m, , whereas the OFES2 estimated a consistent cooling trend below around 200 m, with some exceptions between 500 and –1000 m. Although beyond the scope of this work, the question ofon why both the OFES1 and OFES2 showed relatively consistent warming trends between 500 and –1000 m, around near the depth of the permanent thermocline, necessitatesnecessitate a further work.

—In the Atlantic Ocean, intense warming or cooling extended to deeper regions than inwhen compared to the Pacific Ocean. SpecificallyMore specifically, the strong warming trend in the 1980–90s, estimated from the EN4, appeared extended to as deep as around approximately 750 m,. and On the other hand, moderate warming trend extended to 2000 m since the middle of 1990s in EN4. The OFES1 well captured the warming trend ofin the 1970s and the 1990s, and aalong with the subsequent cooling period in the 2000s, in the upper layer of the Atlantic Ocean when compared to the EN4. However, the OFES1 estimated a strong cooling in the 1980s in the upper layer of the Atlantic Ocean, which was invisible not evinced in the EN4. Interestingly, the OFES1 showed a downward propagation of a strong Atlantic warming trend from around approximately 200 m to approximatelyaround 800 m since the early 1980s;. a Ddownward propagation of the cooling trend from approximatelyaround 600 m to 1800 m before ~1990 can also be seenwas also evinced in the OFES1 data of the Atlantic Ocean (Fig. 11g). Similar to the EN4, a moderate warming trend extended to 2000 m since around the middle of the 1990s in OFES1. As for theIn the case of OFES2, the most prominent pattern that distinguishing distinguished it from the others iswasare the extensive cooling patch before around ~1990 in the upper and middle layers. In addition, it showed a moderate cooling below 1000 m before around 1990. These two extensive cooling patterns in the upper-middle and the deeper lower layers of the Atlantic Ocean, estimated using by the OFES2, raised the following questions: i) what What are the main causes of these two cooling patches exhibited in the OFES2, and ii) why Why they the cooling patches suddenly stopped terminated at around approximately 1990?. One possible reason is thethat improvement of in the reanalysis product of the atmospheric forcing since 1990, especially in the surface HFheat flux and wind stress components, the latter of which has been shown to bebeing proved to be essential forto the subsurface temperature simulations (Kutsuwada et al. 2019).

—In the Indian Ocean, both the OFES1 and OFES2 captured the the warming trend in the 1960–70s and in the 2000s, similar to EN4. However, the OFES1 presented an intense cooling in the upper-middle layer in theduring the 1980s; a similar but less extensive and shallower cooling can also be seen in thewas also evinced in OFES2. Below Beneath the upper layer, the EN4 showed presenteda significantlargelymostly warming in the Indian Ocean, with a major exception of a cooling trend in the 1970s.. In the two OFES, cooling pattern was more prominent than warming below 500 m, especially in OFES2. However, between 500–1000 m, warming patches were seen in the 1960s and after ~1990, in both OFES1 and OFES2.

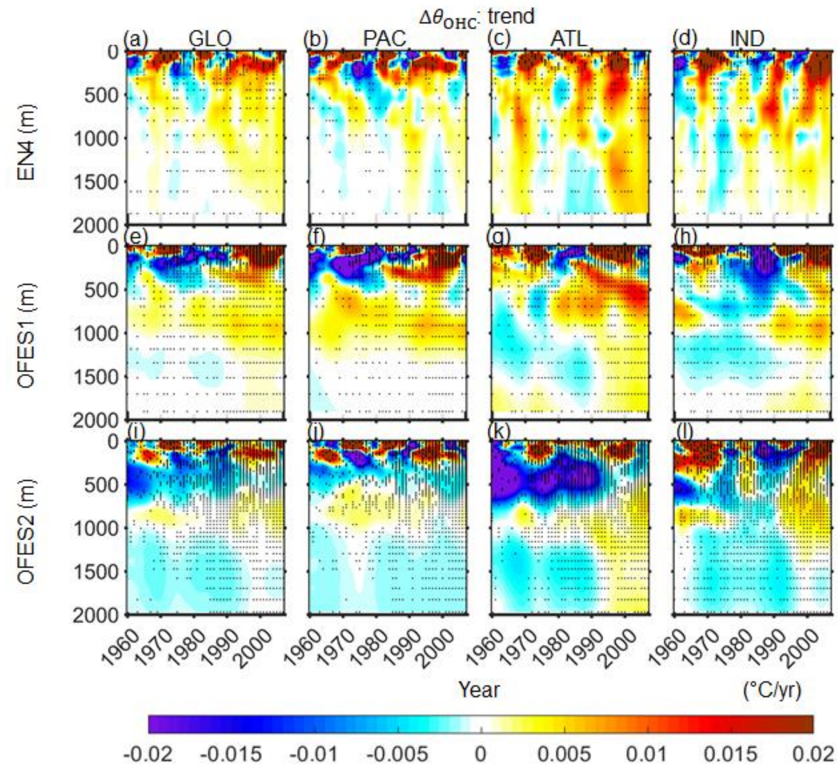

Figure 11. Depth-time patterns of the horizontally averaged potential temperature change $\Delta\theta_{OHC}$ for (left to right) the global, Pacific, Atlantic and Indian Oceans. **Top to bottom:** EN4, OFES1 and OFES2. Horizontal axis: year; vertical axis: depth in m.

Upon comparing Fig. 11 with Fig. 12, it is evinced that ~~To~~ to a great extent, the HV components dominated the OHC variations ~~by comparing the Fig. 12 with Fig. 11~~. For instance, the profound warming and cooling patterns observed in Fig. 11 are~~were~~ mostly associated with the HV component. In addition~~Also~~, the moderate cooling trend observed below 1000 m in ~~the~~ OFES2 was also ~~mainly~~ dominantly related to ~~the~~ HV. Although the SP was generally weaker and less important than the HV in accounting for the OHC variations, its role cannot be ignored. Indeed, intense ~~SP associated~~ warming or cooling episodes associated with the SP component wasere~~were~~ observed~~presented~~ in ~~the~~ EN4 in all ~~the~~ major basins. The increased subsurface SP cooling since the 1990s in the Pacific and Indian Oceans has been~~were~~ particularly interesting~~. One speculation is that this may~~, which could be ~~related~~ associated ~~to~~ with a ~~the~~ significant~~great~~ increase in~~of~~ ~~the~~ subsurface salinity observations since the 1990s. A possible explanation for the appearance of the prominent SP cooling in the Pacific and Indian Oceans, but not in the Atlantic Ocean, is that the Atlantic Ocean has been better observed than the Pacific and Indian Oceans before the 1990s. Another interesting point with regard~~regards~~ to the SP is the consistent SP warming trend that is observed in ~~the~~ OFES2, especially in the Indian Ocean, ~~but~~ and not ~~visible~~ in the other two datasets.

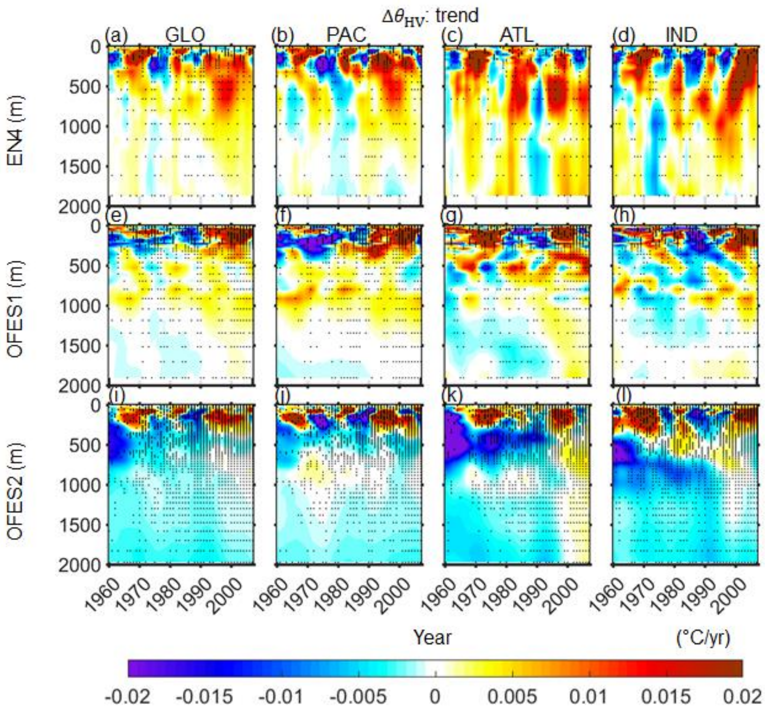

Figure 12. Depth-time patterns of the horizontally averaged potential temperature change from the HV component, $\Delta\theta_{HV}$, for (**left to right**) the global, Pacific, Atlantic and Indian Oceans. **Top to bottom:** EN4, OFES1 and OFES2. Horizontal axis: year; vertical axis: depth in m.

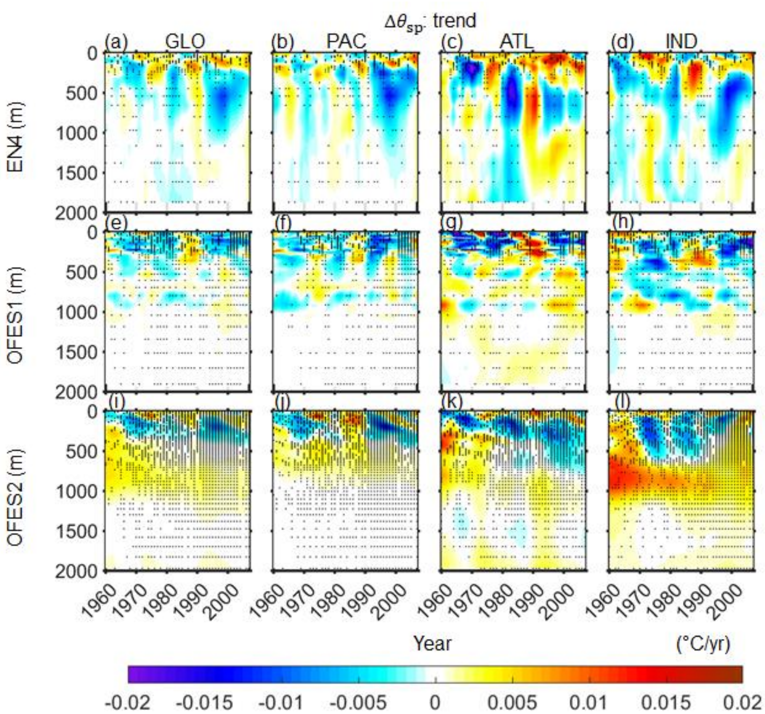

Figure 13. Depth-time pattern of the horizontally averaged potential temperature change from the SP component, $\Delta\theta_{SP}$, for (**left to right**) the global, Pacific, Atlantic and Indian Oceans. **Top to bottom:** EN4, OFES1 and OFES2. Horizontal axis: year; vertical axis: depth in m.

3.~~3~~ 4 Spatial patterns of the potential temperature, HV, and SP trends

To gain a more detailed understanding of the similarities and differences between the trends of potential temperature ~~trends~~ estimated from the three datasets, here we have presented the spatial distributions of the potential temperature change ($\Delta\theta_{OHC}$), and its HV ($\Delta\theta_{HV}$) and SP ($\Delta\theta_{SP}$) components in the three ocean layers (Figs. 14–16).

Upper layer

Warming was almost ubiquitous in ~~the~~ EN4 (Fig. 14a)~~,~~ and was particularly strong in the northern Atlantic Ocean and ~~in~~ the Southern Ocean. These two ~~hotspots of~~ warming hotspots are~~were~~ expected from both theories and models. ~~Specifically~~More specifically, the shallow ocean ventilation in these two regions could generate ~~warm~~ faster warming than the global average (Banks and Gregory 2006; Durack et al. 2014; Fyfe 2006; Talley 2003). Major exceptions of cooling appeared in the Western Pacific ~~Equator~~equator, along the North~~north~~ Pacific Current, in ~~a~~ the meridional band ~~in~~ of the southeastern Pacific Ocean, ~~in~~ parts of the Argentine Basin, and ~~in~~ the southern Indian tropics. All of these cooling regions consist~~consists~~ of a small fraction of the global ocean. ~~As with~~Similar to ~~the~~ EN4, both ~~the~~ OFES datasets showed significant warming in the subtropics, the high latitudes~~high-latitude~~ of the northern Atlantic Ocean, and ~~in~~ the Arabian Sea ~~in~~ of the Indian Ocean. In addition, the OFES1 was similar to ~~the~~ EN4 in ~~showing~~ terms of cooling along the North~~north~~ Pacific ~~Current~~Current. Despite ~~of~~ these similarities, large differences exist between the~~these~~ three datasets. The most significant difference was observed in the Pacific tropics. Although~~, as noted earlier, there~~EN4 indicated the presence of ~~was~~ a zonal band of cooling in the Pacific tropics ~~in the EN4~~, this zonal band, when estimated using ~~in~~ the OFES1 and OFES2 data, was much stronger in intensity and more extensively stretched. ~~and~~It was mainly related to the HV component, especially in the ~~the~~ case of OFES1. ~~These~~ This ~~abnormally~~ strong~~er~~ cooling pattern in the vicinity of ~~Equator~~ the equator ~~were~~ was likely ~~to be resulting~~generated ~~from~~ because of the poor qualities of the atmospheric wind stress over ~~some~~ certain periods. As mentioned earlier, Kutsuwada et al. (2019) demonstrated that the NCEP wind stress used ~~as the~~for forcing ~~of~~ the OFES1 data ~~caused~~generated~~cause~~ a ~~much~~ significantly shallower thermocline in the North~~north~~ Pacific tropical area, and therefore, ~~significant~~ negative differences were observed relative to the observations. In the northeast of the Pacific Ocean, the OFES2, but not the OFES1 and EN4, showed a patch of intense cooling, corresponding to the cooling pattern in the 1960–~~–~~70s (Fig. 8j). The~~the~~ OFES2 also showed four large cooling areas in the Atlantic Ocean (Fig. 14g). In the Indian Ocean, ~~unlike the EN4,~~ the OFES1 and OFES2 datasets indicated the presence of~~there was~~ a patch of intense cooling ~~along the western coast and in the Indian sector of the Southern Ocean. from the OFES1 and OFES2, respectively~~in the southern Indian tropic and in the Indian sector of the Southern Ocean~~.~~ Significant cooling also appeard in the western part of the north Indian Ocean.

—The decomposition of the changes in potential temperature ~~changes~~ into HV and SP components showed that the ~~EN4~~ warming trend, estimated using EN4, was largely the result of isopycnal deepening (HV) in the subtropics. This is consistent with the finding that the subtropical mode water (STMW) is the primary water mass accounting for global warming (Hä~~a~~kkinen et al., 2016), as ~~we be~~also ~~shown~~discussed later. The SP was generally weaker than the HV~~,~~ and tended to counteract the HV warming, especially in the subtropics. This dampening effect can be easily understood from Fig. 1 of Hä~~a~~kkinen et al. (2016). For example, in a stratified ocean with warm~~/~~ and salty water above cold~~/~~ and fresh water, which is typically found in ~~of~~ the subtropics,~~ a pure~~ complete warming of one water parcel can be considered as the~~a~~ vector sum of warming and salination component, manifested as a transition from its original isopycnal to a new isopycnal~~ along its original potential temperature/salinity characteristic~~ (HV part)~~,~~ and a cooling and freshening component along ~~the new~~the original isopycnal (SP). Two major exceptions of the trade-off between HV and SP were the northern Atlantic subtropics and the southern Indian Ocean in EN4, where SP was mostly warming. The SP warming in the northern Atlantic subtropics was generated~~results from~~ owing to a ~~large~~ substantial increase in salinity ~~increase~~ through evaporation (Curry et al., 2003; Hä~~a~~kkinen et al., 2016). Similarly, we found ~~that~~ widespread positive SP warming ~~also occurred~~ in most of the Indian Ocean, except in west to ~~the~~ southwest Australia. Indeed, this SP-related warming in the northern Indian Ocean ~~dominated~~ dominantly controlled the potential temperature change, especially in the Arabian Sea. The most significant SP warming, however, was found in the Indian sector of the Southern Ocean (may be related to the ~~freshening~~ salination of the Southern Ocean), ~~in the~~ southern subtropics of the Atlantic Ocean, and ~~in the~~ Labrador Sea (Fig. 14c).

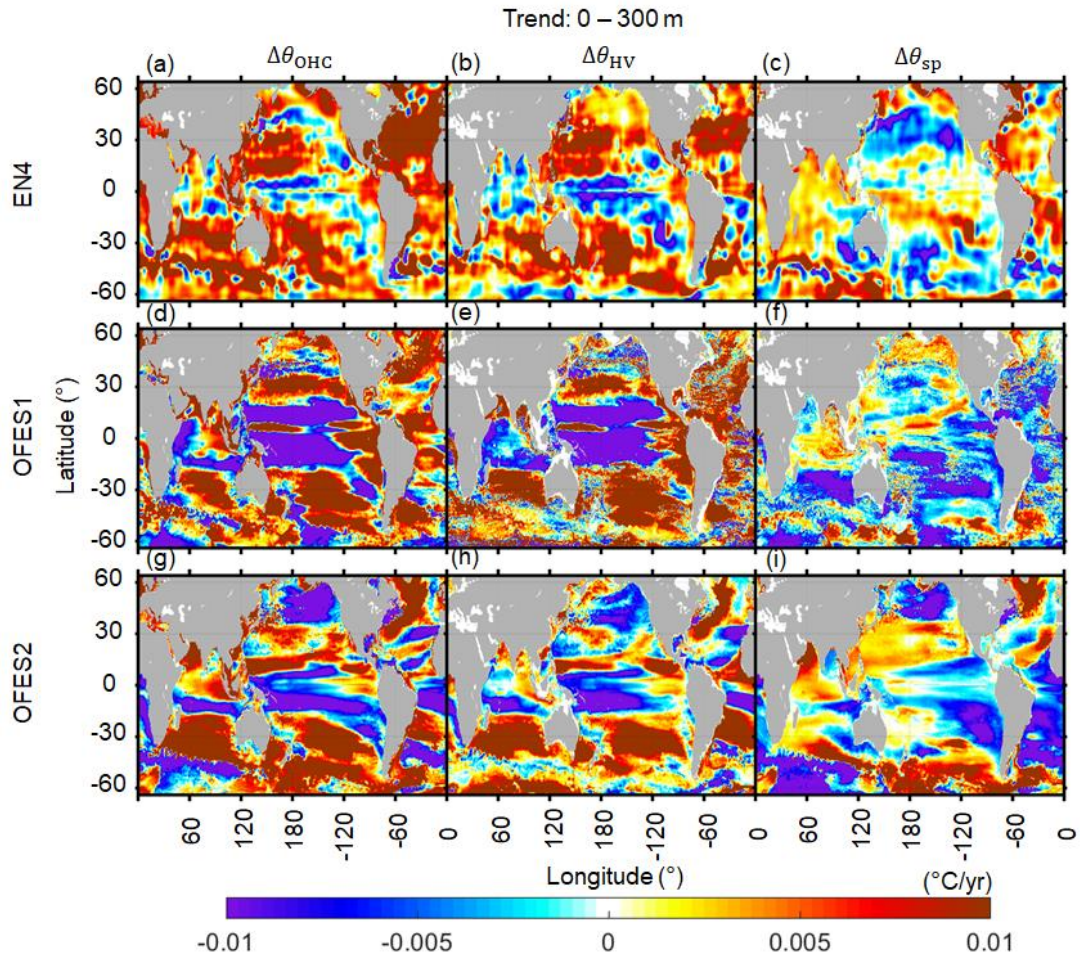

Figure 14. Spatial distributions of $\Delta\theta_{OHC}$ (**top row**), $\Delta\theta_{HV}$ (**middle row**) and $\Delta\theta_{SP}$ (**bottom row**), 1960–2016, in the top ocean layer (0–300 m). Left to right: EN4, OFES1 and OFES2. Standard deviations of $\Delta\theta_{OHC}$, $\Delta\theta_{HV}$ and $\Delta\theta_{SP}$ are given in the Supplementary Information.

Comparing the HV components in the three datasets showed that the two OFES simulations were able to reproduce the subtropical HV warming pattern, although less accurately in the northern Pacific subtropics. The strong and extensive equatorial cooling in the Pacific and Indian Oceans was largely associated with variations in ~~the~~ HV in the two OFES datasets.

The SP in the OFES1 was similar to ~~the~~ EN4 in the northern subpolar region of the Pacific Ocean, ~~in~~ parts of the northern Pacific subtropics, ~~in~~ the Labrador Sea, and ~~in~~ parts of the northern Indian Ocean. The ~~OFES2~~ SP, estimated using OFES2, was similar to the estimates from the EN4 in the Labrador Sea and the western Indian Ocean. In general, however, ~~there arewere~~ no common patterns were observed in most of the global oceans~~ocean~~. In particular, neither of the OFES datasets captured the SP warming in the northern Atlantic subtropics, and the OFES2 dataset indicated moderate SP warming in the North~~north~~ Pacific subtropics and intense SP warming in the Pacific sector of the Southern Ocean, respectively. The improvements in~~of~~ SP determined based on ~~from~~ the OFES2 dataset over that from the OFES1 in the Arabian and Indonesian seas,~~Seas~~ ~~but~~ and not in the Bengal Bay, ~~was~~ is partly consistent with ~~the~~ S2020~~, to some extent~~. The authors demonstrated a smaller bias in the water-mass properties ~~in~~ of the Arabian and Indonesian seas~~Seas~~, ~~but~~ however, a large salty bias remained in the Bengal Bay in the OFES2.

In Fig. ~~3~~2, we show~~showed~~ that the SP, estimated using EN4 and OFES2, was ~~highly~~ largely similar ~~between the EN4 and OFES2~~ in the upper layer of the Pacific Ocean. However, the spatial distributions of the SP component in the Pacific Ocean were seldom~~seldomly~~ similar between ~~the~~ EN4 and OFES2. In other~~That~~ words~~is~~, the time series of a basin-wide quantity hides many details.

Middle layer

~~The~~ EN4 showed that the cooling ~~in~~ of the ~~the~~ ocean~~,~~ was mostly concentrated in the southern Pacific subtropics~~,~~ and ~~in~~ the region associated with the Kuroshio (Fig. 15a). Clear warming trend was observed, accompanied by sporadic cooling patches ~~For~~ in the rest of the global ocean, especially over ~~the bulk~~ most of the Atlantic Ocean, in the northern Indian Ocean, and along the Antarctic Circumpolar Current (ACC) path ~~in~~ of the Southern Ocean~~,~~. ~~clear warming was observedpresented, accompanied by sporadic cooling patches.~~ The OFES1 dataset could reproduce some warming patterns in the northern Pacific Ocean, the bulk of the Atlantic Ocean, ~~in~~ the eastern part of the northern Indian Ocean, and parts of the ACC path. However, notable differences were~~can be~~ found between ~~the~~ OFES1 and EN4. Among these differences, the most prominent is the intense cooling in the southern Indian Ocean as estimated from OFES1, which correspondes to the cooling during the 1990s, ~~as estimated from the OFES1, which was found to occur in the 1990s, as shown in from~~ (Fig. 3~~(~~d~~)~~). In addition, strong cooling patches were also found in the southern Pacific tropics, west to ~~the~~ central-south America, in the northern Atlantic subtropics, in the Arabian Sea, and along parts of the southern edge of the ACC in OFES1. The pattern in the OFES1 Pacific Ocean clearly appears as zonal bands;~~,~~ ~~but~~ however, this zonal strip -was obscure in ~~the~~ EN4. Consistent with Fig. 3, intense cooling was simulated by OFES2 ~~in~~ for all ~~the~~ major basins ~~by the OFES2~~, with the most prominent ~~in~~ being in the Atlantic Ocean. Large-scale ~~strong~~

warming patterns were found in the Kuroshio region, in the southern Pacific and Indian subtropics, in the northern Atlantic Ocean (north ~~to~~ of 35° N), in the western part of the northern Indian Ocean, and in the Pacific and Atlantic sectors of the Southern Ocean. In general, ~~over the bulk of the global ocean,~~ there were apparent differences between the~~se~~ three datasets ~~over~~when the bulk ~~of the~~ global ocean was considered. The above 700 m ~~was~~ is relatively well observed, especially in the Atlantic Ocean (even back to 1950–60s, Hä~~a~~kkinen et al., 2016). Therefore, it is likely that the OFES2 dataset was an~~the~~ outlier at ~~this~~ the analyzed multi-decadal scale, and there ~~were~~ could be some potential problems in the OFES1, for example, in the southern Indian Ocean.

~~—~~Interestingly, EN4 suggested that ~~the~~ HV warming was almost ubiquitous in the middle layer ~~from the EN4~~ (Fig. 15b), especially in the southern hemisphere~~Southern Hemisphere~~, which is consistent with the warming shift toward~~towards~~ ~~to~~ the s~~S~~outhern h~~H~~emisphere ~~found in~~~~(~~ Hä~~a~~kkinen et al., ~~(~~(2016). Correspondingly, ~~the~~ SP cooling also occupies most of the global ocean (Fig. 15c), with a similar southern shift, the most prominent ~~to~~ being along the east and western regions of ~~the~~ Australia. ~~The~~ Major~~major~~ SP warming patches were found in the Sea of Okhotsk, north of~~to~~ the Gulf Stream, in the Arabian Sea, and along the southern edge of the ACC. These regions are generally associated with strong variations in salinity ~~variations~~. Comparing ~~the~~ HV and SP ~~between~~ estimated based on the EN4 and OFES1 dataset showed that the OFES1 captured some warming patterns in the Pacific and Atlantic, ~~but~~ and not in the Indian~~,~~ subtropics. The ~~HV~~ agreement of HV ~~in~~ for the southern Pacific ~~and~~, Indian tropics, and ~~in~~ the Southern Ocean was~~were~~ mostly poor. ~~As for the~~In the case of SP, the OFES1 reproduced ~~the~~ intense SP cooling in west ~~to~~ ern ~~the~~ Australia and ~~in~~ the southern Pacific subtropics, despite its~~of~~ smaller coverage compared to ~~the~~ EN4. However, ~~the~~ OFES1 showed almost opposite trends of SP ~~trends~~ over most of the global ocean. In ~~the~~ OFES2, both ~~the~~ HV and SP were strong, ~~but~~ however, the basin-wide cooling was mainly ~~the~~ generated as a result of HV. Overall, the OFES2 dataset had a reasonable agreement with ~~the~~ EN4 in the southern subtropics (Pacific and Indian Oceans) in terms of HV. It also had a common HV warming patch in the northern Atlantic Ocean (north to 35° N) as ~~the~~ EN4. With regard~~regards~~ to ~~the~~ SP, the OFES2 was similar to ~~the~~ EN4 in ~~showing~~ displaying SP warming in the Arabian Sea and parts of the southern edge of the ACC. In addition~~Also~~, it also captured ~~the~~ SP cooling in the eastern Pacific Ocean, along the Gulf Stream path, west of~~to~~ ~~the~~ Australia. Except for~~of~~ these similarities, however, ~~the~~ OFES2 dataset was generally ~~opposite~~ not consistent ~~to~~ with that of ~~the~~ EN4.

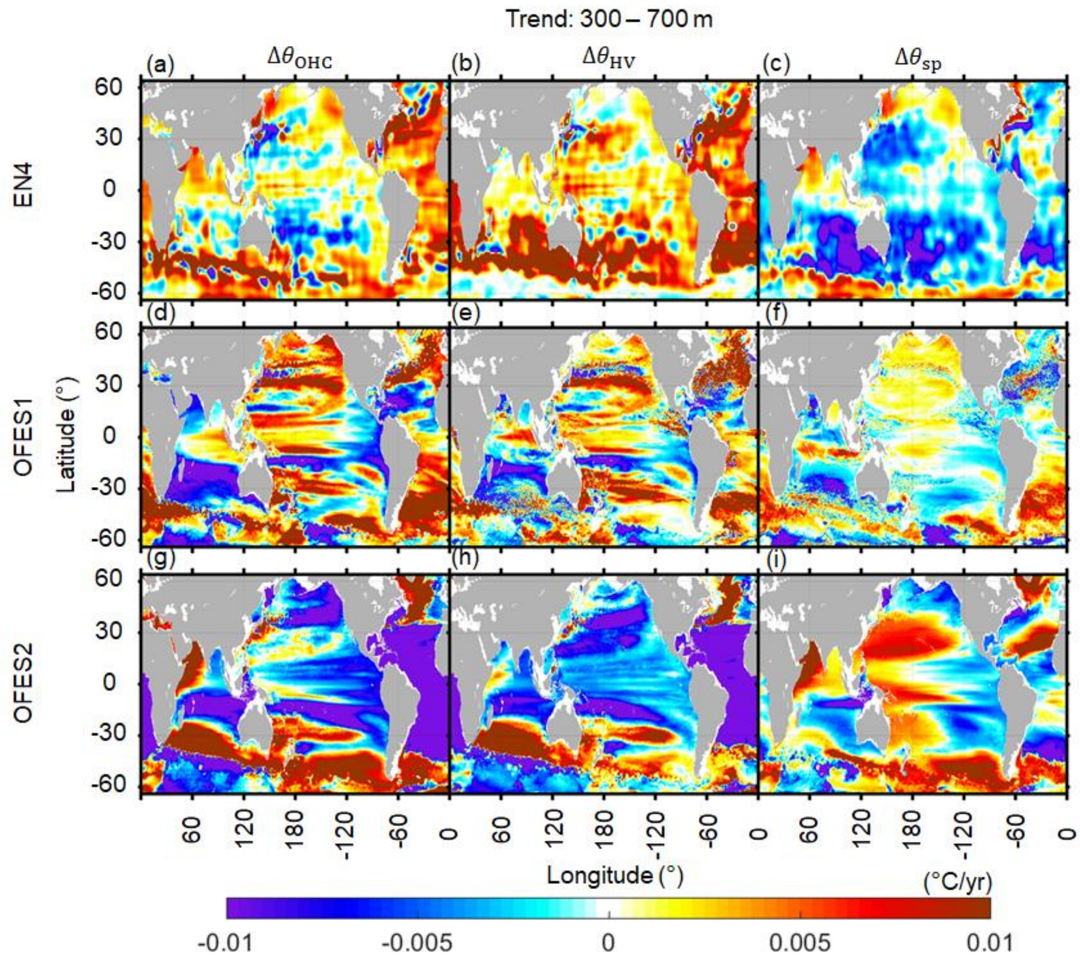

Figure 15. As for Fig. 14 but for the middle layer (300–700 m).

Lower layer

~~The~~ In general, the warming and cooling intensities were ~~generally much~~ significantly weaker in the lower layer ~~than~~ compared to that in the top two layers, which is consistent with ~~many~~ several previous findings that more ocean heat ing occurs in the upper 700 m than at greater depths (Häakkinen et al., 2016; Levitus et al., 2012; Wang et al., 2018; Zanna et al., 2019). ~~The~~ EN4 showed widespread warming patches in the Southern and Atlantic Oceans, and ~~as well as in the~~ three large zonal bands of cooling in the southern subtropics of the Pacific and Indian Oceans, and in the northern subpolar region of the Atlantic Ocean (Fig. 16a). Similar to ~~the~~ EN4, the OFES1 dataset reflected warming ~~was observed~~~~seen~~ along the northern edge of the ACC and in the southern Atlantic Ocean ~~in the OFES1~~, ~~but~~ although the intensity of warming was much stronger ~~with a much stronger intensity~~for OFES1 than in ~~the~~ EN4 (Figs. 16a, d). In addition, OFES1~~There was~~ also reflected moderate warming over almost the entire~~whole~~ Pacific Ocean. ~~in the OFES1.~~ Significant differences between ~~the~~ OFES1 and EN4 were found in the northern Atlantic Ocean, where the OFES1 showed extensive cooling compared to the moderate warming in ~~the~~ EN4. OFES1 ~~There was also~~demonstrated strong cooling in the ~~OFES1~~ Arabian Sea, which is in contrast to the quite weak warming of the ~~in the EN4~~ Arabian Sea obtained from the EN4. To some extent, the OFES2 was similar to the other two datasets in showing warming along the northern edge of the ACC and in the southern Atlantic Ocean, south to 30 °S (Fig. 15g), despite ~~of~~ the ~~intensity~~ differences in the intensity of warming. It also showed cooling in the low and middle latitudes of the Atlantic Ocean, ~~as did the~~similar to OFES1 but ~~opposite~~ unlike ~~to the~~ EN4. However, the bulk of the Pacific Ocean was shown to be cooling in the OFES2, which was almost opposite to the OFES1 results (Fig. 15d) and ~~only~~ similar to ~~the~~ EN4 only in parts of the southern Pacific subtropics (Fig. 15a). Moreover, OFES2 reflected intense and widespread cooling ~~was observed~~appeared in the Indian sector of the Southern Ocean ~~in the OFES2~~. The warming of the northern ACC was captured by the OFES2.

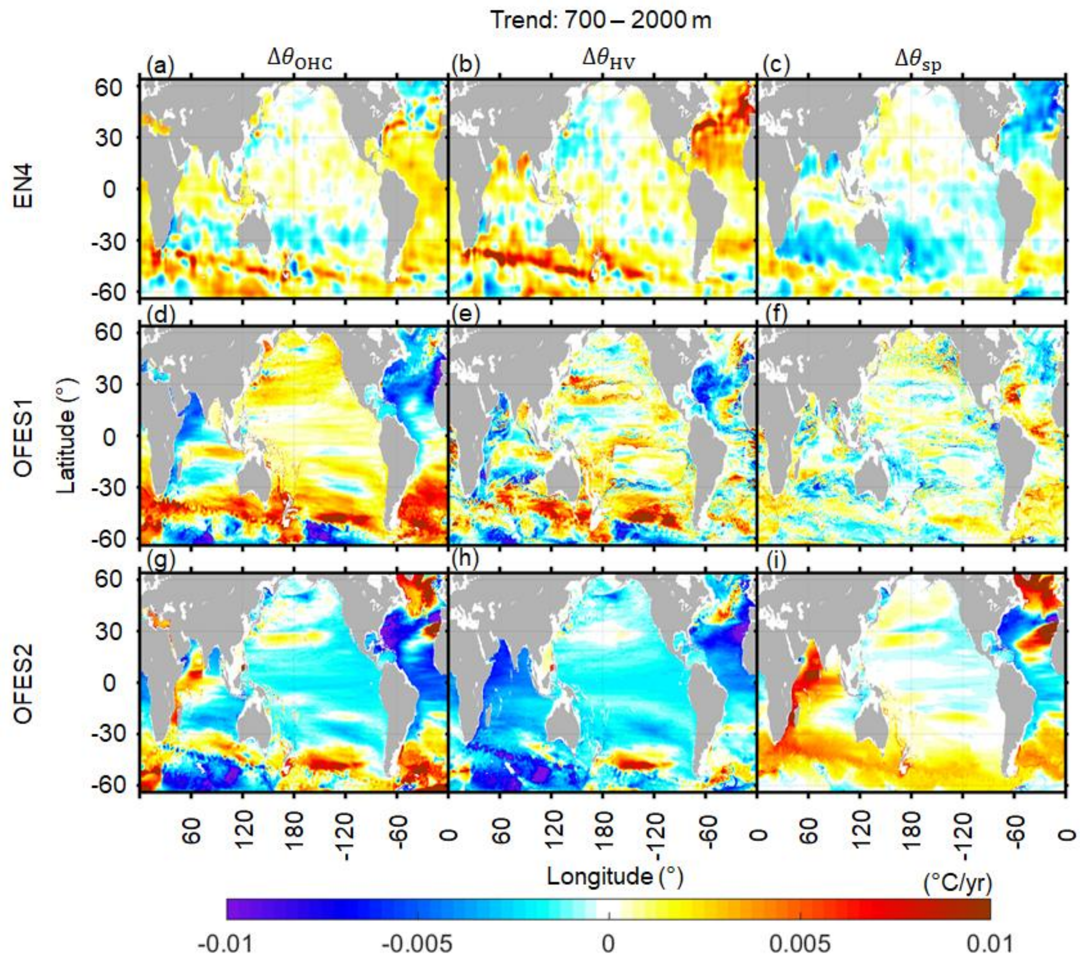

Figure 16. As for Fig. 14 but for the lower layer (700–2000 m).

—In ~~the~~ NE4, there was intense HV warming along the northern edge of the ACC in the Indian and Pacific Oceans, and in the northern Atlantic Ocean (Fig. 16b), which largely accounted for the total potential temperature variations. ~~and~~ HV warming was~~were~~ generally accompanied by SP cooling (Fig. 16c). Moderate HV and SP warming coexist in~~In~~ the northern Atlantic tropics and the southern Atlantic Ocean~~, moderate HV and SP warming coexist~~. We found that the OFES1 captured the HV warming pattern along the northern edges of the ACC, which is~~being~~ consistent with the results from ~~the~~ EN4. However, there were remarkable differences in OFES1 results from those~~at~~ of ~~the~~ EN4, particularly in the northern Atlantic and Indian Oceans. ~~As for the~~In terms of SP, there were some similarities between the OFES1 and EN4;, for example, they both had SP cooling and warming in the northern and southern Atlantic Ocean, respectively. Among the three datasets, the OFES2 showed the most extensive and strong HV-associated cooling component, but although there was a generally cooling in thetrend HV component, except for a patch of HV warming in the Pacific sector of the Southern Ocean, and whichsuch a warming patch was also seen observed in the EN4 dataset. In contrast,The -OFES2 estimated intense SP warming was estimated in the OFES2 in the Southern Ocean, in the western Indian Ocean, and in the northern Atlantic subpolar regions., and aA large-scale patch of abnormally strong SP warming, associated with the Mediterranean Overflow Water (MOW), was also observed. This extremelyvery strong SP warming, related toassociated with the MOW, is likely the result of the unrealistic spreading of the salty Mediterranean overflow found reported in **S2020**.

—Besides the above-discussed multi-decadal linear trends, we have demonstrated that (not shown here) the significant differences between the two OFES datasets and the EN4 were significantlymuch reduced if we considered only the period between 2005 and –2016 is only considered, during which was the two OFES has beenwere argued to be well spun-up by (**S2020**). In addition, over this 12-year periodese 12 years, the spatial pattern of the OFES2 showeddid show some improvements over the OFES1 for the upper and middle layers, but however, it was not necessarily true for the lower layer, when taking the EN4 was used as a reference. Does Is this better agreement come a result of from a better spun-up or come it was generated from owing to the improvements inof the reanalysis product of the atmospheric forcing for these two OFES data? This interesting question requireswould require a further detailed exploration in the future.

3.54 Trends in of the HV and SP in the neutral density domain

To analyzeanalyse the warming and cooling from the perspective of water masswater-mass, iPlotting thet is useful to show the HV and SP components in neutral density coordinates provides useful information to analyze the warming and cooling from the perspective of water--mass, as suggested by one reviewer. Following Häakkinen et al. (2016), we calculated the linear trend (over 1960–2016) inof the zonal-averaged sinking of the neutral density surfaces in each major basin over 1960–2016 (Fig. 17) and also the SP-related warming or cooling along the neutral density surfaces (Fig. 18).

—Our results, based on the EN4 dataset, were similar to those of Häakkinen et al. (2016), using the EN4, although they used who used an earlier version of EN4 version dataset (i.e., EN4.0.2) and considered the period fromover 1957 to –2011. More sSpecifically, our EN4 results similarly showed that the bulk of HV warming (deepening of neutral density surfaces) was associated with a water--masswater-mass of over 26 kg/m^3, and was mainly concentrated south to of 30° S, to wit, from the ventilation region at high latitudes to the subtropics. There was one exception in the Atlantic Ocean, where warming also occurred at– lowththe middlelow-middle latitudes and in the northern Atlantic Ocean. The concentrated warming in the northern Atlantic Ocean was attributed to the phase change of the North Atlantic Oscillation (NAO) from negative in the 1950–60s to positive in the 1990s (Häakkinen et al. 2016; Williams et al. 2014). As explained byin Häakkinen et al. (2016), thethese significant deepening of neutral density surfaces waswere associated with the sSubtropical mMode wWater (STMW, 26.0 < σ_0 (kg/m^3) < 27.0) and the Subantarctic Mode Water (SAMW, 26.0 < σ_0 (kg/m^3) < 27.1). These vertical displacements of neutral density surfaces may probablyhave resulted from heat uptake via subduction, which then subsequently might have spread from these high-latitude ventilation regions. The large vertical deepening of the STMW and SAMW would had then subsequently pushed the Subpolar Mode Water (SPMW, 27.0 < σ_0 (kg/m^3) < 27.6) and the Antarctic Intermediate Waters (AAIW, 27.1 < σ_0 (kg/m^3) < 27.6) further down. However, as the vertical displacement of the STMW/SAMW was larger, its volume would have therefore increased, and the volume of the underlying SPMW/AAIW had decreased (Häakkinen et al., 2016). Besides these significant sinking of neutral density surfaces, there was generally a shoaling pattern of lower density (σ_0 (kg/m^3) ranging from 24 to –26), and which was mostlyainly concentrated between the equatorEquator and 30° S. To a large extent, this shoaling occurred in the central water, for example, in the South Pacific Central Water (SPCW).

Here, our focus is not on theIn this study, we have not focused on the detailed mechanisms of warming from the perspective of water mass, as it was done in previous studies Häakkinen et al., 2016 (). Instead, we have focused on the differences between the three datasets in thewith respect to the trends of the HV and SP.

It can be seen that along the surfaces of the Pacific and Indian Oceans, there was a generally an appearanceapperance of HV warming in almost all the three datasets. In the Atlantic Ocean, however, the EN4 estimated a sea surface cooling south to of 30° S and in the northern tropics; the OFES2 also estimated a cooling trend near the surface of the Atlantic tropics. In contrastDifferent tofrom both the EN4 and OFES2, the OFES1 showed an intense HV cooling pattern along the Atlantic surface between around 30 and –50° N (Fig. 17e).

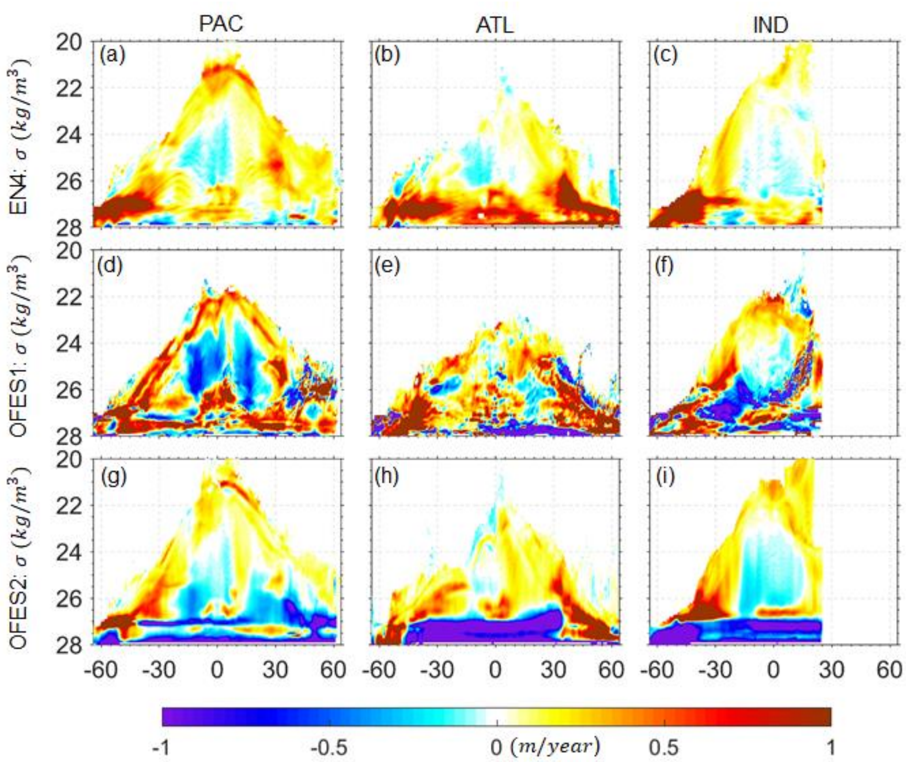

Figure 17. Linear trends in the zonal-averaged sinking of the neutral density surfaces in the Pacific (**left column**), Atlantic (**middle column**) and Indian (**right column**) Oceans. **Top to bottom:** EN4, OFES1, OFES2. Positive values mean deepening of the neutral density surfaces. The calculation was for the water above 2000 m.

—South to of 30° S, EN4 detected large downward movements, associated with the STMW, SAMW, and AAIW were found in all the three basins in the EN4;. Inin the the case of OFES1, the dominant pattern in the three basins was sinking, however, but it was surrounded by shoaling patches; larger differences from the EN4 were found in the OFES2, which showed significant and extensive shoaling patterns, especially in the Indian Ocean. The almost opposite trend in the vertical displacements of the neutral density surfaces between the OFES2 and the observation-basedobservational-based EN4 may indicate that the properties of water-mass properties simulated in the OFES2 were unrealistic, at least at this multi-decadal scale.

—In the ocean interior between 30°S and 30° N, the OFES1 presented shoaling patterns in the Pacific and Indian Oceans, but however, such pattern was not prominent in the Atlantic Ocean. Although thesese shoaling patterns in the Pacific and Indian Oceans were also seen evinced in the EN4, as noted earliereailer, their magnitude in the EN4 was generally much significantly smaller. -The OFES2 had a better agreement with the EN4 in for the shoaling pattern in the southern Pacific subtropics. EN4 It also captured the shoaling in the EN4 Indian Ocean, with a similar coverage, however, the intensity wasbut generally stronger. The Shoalingshoaling in the southern Atlantic subtropics was not typically found in the OFES2, similar to the OFES1, but different from the EN4.

—In the nNorth to of 30° N, EN4 detected widespread sinking was widespread in the EN4, particularly strong in the northern Atlantic Ocean. This very strong sinking in the northern Atlantic Ocean originatedcame mainly from the SPMW and STMW. In the EN4 Pacific Ocean, there werewas certainsome shoaling patches, which werewas related to the North Pacific Intermediate Water (NPIW), and to a large extent, corresponded to the HV cooling in (Fig. 16(b)). In the OFES1, the pattern was filled with both sinking and shoaling patches, and which defies easy interpretationintepretation. However, an apparent outlier of OFES1wasis the intense shoaling in the OFES1 northern Atlantic Ocean (mostlyainly below 700 m (from Figs. 14–16)), which isjust the opposite ofto the EN4. The shoaling of neutral density surfaces in the OFES2 Pacific Ocean, north to 30° N, was even more prominent than that in the OFES1. The OFES2 had a better agreement with the EN4 in terms of thehe sinking patterns in the Atlantic Ocean north to of 30° N.

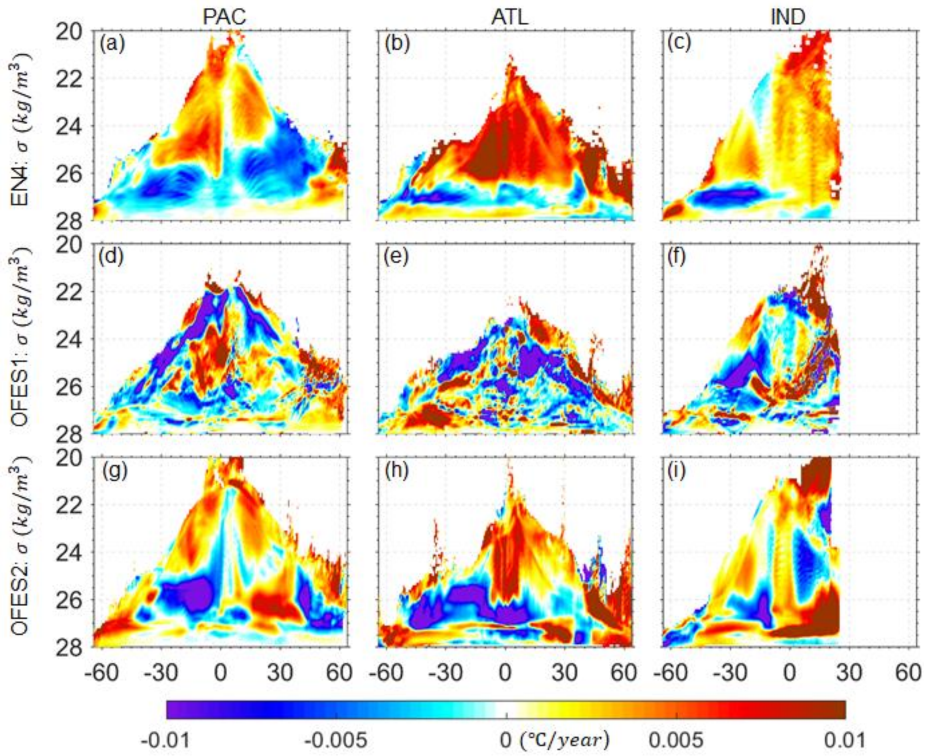

Figure 18. Linear trends in the zonal-averaged warming or cooling along the neutral density surfaces in the Pacific (**left column**), Atlantic (**middle column**) and Indian (**right column**) Oceans. **Top to bottom:** EN4, OFES1, OFES2.

—The major SP warming episodes determined by~~in the~~ EN4 in the Pacific Ocean ~~was~~ were associated with ~~the~~ STUW and Pacific Central Water (PCW) in the low and middle latitudes, with a shift toward~~towards~~ ~~to~~ the southern hemisphere~~southern hemisphere~~. The northern high-latitude SP warming was mainly related to the Pacific Subarctic Intermediate Water (PSIW). The two SP coolings~~cooling~~ ~~came~~ were generated from the STMW, corresponding to the ~~sinking pattern~~isopycnal deepenings in Fig. 17(a). ~~This~~ HV warming~~-~~/ SP cooling was particularly typical in the subtropical regions, and ~~the~~ HV ~~warming~~ / SP warming was typical in the subpolar regions, ~~as noted above, and~~ more details of which are~~were~~ presented in Hä~~a~~kkinen et al. (2016). ~~Very~~ An extremely strong SP warming trend occurred in the Atlantic Ocean, resulting from salination via ~~the~~ evaporation~~process~~. In the southern Atlantic Ocean, the pattern of SP cooling ~~is~~ was mostly associated with the sinking of the STMW.

—The SP pattern determined from the OFES1 dataset was quite noisy, and generally had~~had generally~~ a poor agreement~~agreements~~ between ~~the~~ OFES1 and ~~the~~ EN4 in terms of SP warming, which is likely to result~~be resulting~~ from some issues of salinity simulation in the OFES1. As shown in **S2020**, ~~the~~ OFES1 was not capable of simulating salty outflows, for example, the outflow through the Persian Gulf into the Indian Ocean. There were notable improvements in the salinity field~~in~~s of ~~the~~ OFES2 over OFES1, which has been mainly attributed to the inclusion of river runoff and ~~a~~ sea-ice~~model~~, ~~but~~ however, some issues associated with~~still remained, such~~e.g.~~as,~~ poor performance in the simulation of the Mediterranean outflow remained. Overall, the SP warming pattern in the density coordinate was significantly improved in ~~the~~ OFES2 ~~when~~ compared to ~~the~~ OFES1. However, ~~when~~~~When~~ upon combining~~combing~~ Figs. 14–16~~, however~~, ~~one can see~~it is evinced that the similarities in ~~the~~ SP estimation between the OFES2 and ~~the~~ EN4 dataset ~~was~~ were confined to a small fraction of the global ocean, mainly in the upper and middle layers of the Labrador Sea~~ and~~ , ~~the~~ northern Indian Ocean, and ~~in the~~ Southern Ocean. In addition, the simulations by OFES2 ~~was also~~shared similarities with those of ~~similar to the~~ EN4 in showing a patch of SP cooling in the western part of the northern Atlantic subtropics.

3.~~5~~ 6 A basin-wide heat budget analysis

The fundamental mechanisms controlling the oceanic thermal state include the net surface HF~~heat flux~~, ~~the zonal~~ ZHA and MHA~~meridional heat advectionadvections~~ in the horizontal direction, and ~~the~~ VHA~~vertical heat advection~~ and ~~diffusion~~ VHD in the vertical direction (Fig. 1b). Lateral heat diffusion was not considered here~~, as~~ because it was found to play a minor role in~~from~~ our analysis (not shown). Because~~Since~~ our focus is on the global and basin-wide OHC in the three vertical layers, we calculated and compared the inter-basin heat exchange, and the VHA~~vertical heat advection~~ and ~~diffusion~~VHD, integrated over each basin from 1960 to –2016.~~-~~ No vertical heat diffusivity data were available from ~~the~~ OFES1~~, and~~. In addition, the vertical heat diffusivity data from ~~the~~ OFES2 were~~as~~ temporarily unavailable because~~due~~ of~~to~~ a security incident when this manuscript was prepared. This prevented us from directly calculating and comparing the ~~the vertical heat diffusion~~VHD between OFES1 and OFES2 ~~directly~~. As an alternative, we calculated the residual of the OHC change, along with ~~and~~ all ~~the related~~associated heat transport components that contribute ~~in~~to each basin, and used~~took~~ the results~~it~~ as a proxy for ~~the~~ vertical diffusion. This indirect method ~~may~~ might suffer from some errors;~~,~~ for instance, it includes the impacts of river runoff in the OFES2, ~~but~~ however, it can still provide us with some ~~with~~ important information. ~~-~~The~~Our~~ calculations are listed in Tab~~Tabs.~~le 2–4. The related time series of these surface heat fluxes~~flux~~ and heat advection are~~were~~ shown in ~~the s~~Supplementary Figs. S7–9.

Upper layer

In the Pacific Ocean, the ~~changing~~ rate of change of the ~~time-averaged~~ OHC was rather low for~~in~~ both ~~the~~ OFES1 and OFES2. However, the average~~d~~ surface HF~~heat flux~~, estimated using the ~~in~~ ~~the~~ OFES1 dataset, was twice ~~tha~~that of~~t~~ ~~in the~~ OFES2, indicating that more heat was injected into~~to~~ the OFES1 Pacific Ocean,~~ and~~ signifying the differences in ~~the~~ atmospheric forcing. Vertically, both datasets indicated a net downward advection of heat in the Pacific Ocean at 300 m, ~~but~~ however, the intensity was much stronger ~~intensity~~ in the OFES1 (different by approximately~~around~~ 0.7 W/m^2),~~;~~ which~~this~~ may be related to their different wind-forcing sources, as the downward heat advection in the upper ocean was mainly from the wind-driven Ekman pumping in the subtropical gyres. Indeed, Kutsuwada et al. (2019) claimed that the NCEP wind stress curl was too strong, and ~~caused~~ had generated the overly strong Ekman pumping. There ~~was 0.150 W/m^2 more~~ was an increase in the eastward heat advection through the water passage between the Australian mainland and 64° S by 0.150 W/m^2 (P3 in Fig. 1a) in the OFES2, in a comparison to the OFES1. Although the two OFES datasets indicated that the MHA from the Southern Ocean to the Pacific Ocean~~Oceans~~ (P4) had~~was of~~ opposite signs~~sign in the two OFES datasets~~, the relatively small absolute value indicated that this difference was ~~slight~~minor. The Drake Passage (P5) is the major water passage, through which heat is exchanged between the Pacific and Atlantic Oceans. There was 0.108 W/m^2 more heat loss through ~~the~~ P5 into the Atlantic Ocean in the OFES1, inferring a stronger ACC from the OFES1 in the upper ocean. ~~The~~ P7 and P8 connect the Pacific and ~~the~~ Indian

Oceans,~~;~~ and the Indonesian Throughflow (ITF) flows through ~~the~~ P7. The MHA passing through ~~the~~ P7 was almost ~~tw~~one time~~s~~ stronger in ~~the~~ OFES2 than in ~~the~~ OFES1, with a difference of 0.637 W/m^2. This indicated an enhancement of the I~~F~~TF simulated by the OFES2, which, to some extent, agreed ~~well~~ with the results of Sasaki et al. (2018), who showed that the inclusion of a tidal-mixing scheme resulted in an intensification of the ITF, ~~remembering~~ noting that the ~~a~~ tidal-mixing scheme was implemented in ~~the~~ OFES2 and~~but~~ not in OFES1. In addition, the OFES1 demonstrated that~~showed~~ more heat was transported westward into the Indian Ocean between Papua New Guinea and Australia (P8), ~~but~~ however, the small absolute heat advection indicated that it was not the major cause of the OHC discrepancy between ~~the~~ OFES1 and OFES2. The net heat advection through the Bering Strait (P9) was rather weak in both datasets. The indirect calculation of the VHD showed that there was net downward heat diffusion at a depth of 300 m in the Pacific Ocean in both the ~~two~~ OFES datasets, although the intensity was much ~~but with a much~~ stronger ~~intensity~~ (~~different by~~ 0.747 W/m^2) in the OFES1.

~~—~~In the Atlantic Ocean, the OHC increased at an average rate of 0.032 W/m^2 in ~~the~~ OFES1 ~~but~~, however, it decreased by 0.014 W/m^2 in ~~the~~ OFES2. There was net surface heating in the OFES1 Atlantic Ocean, but minor cooling was evinced in the OFES2. The two OFES datasets were also profoundly different in ~~the~~ terms of VHA at 300 m. Specifically, ~~the~~ OFES1 showed a net downward heat advection, and~~the~~ OFES2 showed~~an~~ upward and ~~much~~ significantly weaker heat advection. Again, this difference in the VHA was likely the result of different wind stress datasets in the two OFES, as discussed above. In a comparison to the OFES2, ~~T~~the OFES1 showed an increase in the ~~0.158 W/m^2 more~~ heat transported from the Atlantic Ocean to the Indian Ocean through ~~the~~ P1 between ~~the~~ South Africa and 64° S by 0.158 W/m^2. As mentioned above, more heat was advected into the Atlantic Ocean through the Drake Passage (P5) in the OFES1. Additionally, there was more heat advected southward from the Atlantic Ocean to the Southern Ocean in ~~the~~ OFES1 (P6). The wide passage connecting the North~~north~~ Atlantic Ocean to the Arctic Ocean (P10) ~~also~~ served as the major channel, through which the Atlantic Ocean exchanged heat with the Arctic Ocean; the two OFES datasets exhibited~~gave~~ similar heat loss. All these differences ~~combined~~ led us to conclude that the ~~respective values for the~~resulting ~~vertical heat diffusion~~ VHD at 300 m differed by 0.411 W/m^2 (~~more~~ with ~~a trend of increasing~~stronger upward heat diffusion estimated by~~in~~ the OFES1).

~~—In~~ For the Indian Ocean, the average~~averaged~~ ~~OHC increasing~~ rate of increase in OHC, calculated by OFES2, ~~-~~was ~~0.009 W/m^2~~ higher ~~in the OFES2~~ than in ~~the~~ OFES1 by 0.009 W/m^2. The time-averaged surface HF~~heat flux~~ in ~~the~~ OFES2 was 0.729 W/m^2 lesser than that in ~~the~~ OFES1. Both datasets showed a net downward heat advection, ~~but that~~however, the results obtained from ~~in the~~ OFES2 ~~was~~ were approximately~~around~~ ~~three~~ two times stronger. The small difference in the southward heat advection across ~~the~~ 64° S (~~the~~ P2) only affected the OHC in the upper Indian Ocean to a small extent. In contrast, the differences in the HF, VHA, and ~~the~~ MHA associated with the ITF contributed to the difference and led us to calculate a remarkable ~~discrepancy~~ difference of 1.898 W/m^2 in the VHD at a depth of 300 m in the Indian Ocean. The enhanced ITF is one of the main contributors to the larger increase of the OHC ~~increase~~ in the upper layer of the OFES2 Indian Ocean (Fig. 2).

~~—~~To summarize, OFES1~~there was~~ estimated ~~a generally more~~ higher surface HF~~heat flux~~ into the major basins ~~in the OFES1~~. The VHA~~vertical heat advection~~ was generally downward, indicating the essential role of ~~the~~ subtropical Ekman pumping in the heat uptake ~~in~~ of the upper ocean layer. The differences between~~of~~ these two (HF and VHA) contributors were mainly due to~~from~~ the different atmospheric forcing used in the two OFES datasets, emphasizing the importance of reliable atmospheric forcing products~~product~~ in ~~the~~ numerical ocean model~~l~~ling. Although the different wind stresses~~stress~~ could also produce different lateral advections through ~~the~~ P1–P10, the local-integrated differences were generally smaller than the basin-integrated differences. The most prominent difference in the ~~the~~ lateral heat advection was associated with the ITF, which was mainly ~~as~~ a result of the adoption of a tidal-mixing scheme. This ITF-related difference and the indirectly inferred VHD suggested the significance of the vertical mixing scheme in producing the examined differences in~~of~~ OHC.

Table 2. Time-averaged OHC, surface heat flux (HF) and advection of heat through the major water passages for the upper layer (0–300 m) of each basin ~~(0–300 m)~~. VHA in this table is at a depth of 300 m. Residual: difference between the OHC increase and all the heat flux into a basin, approximately the ~~vertical diffusion of heat~~VHD. All quantities converted to W/m^2 applied over the entire surface of the Earth. Values smaller than 0.001 are set to 0. Positive means heat gain and negative means heat loss.

PACIFIC OCEAN (0–300 m)

	OHC	HF	VHA	P3	P4	P5	P7	P8	P9	Residual
OFES1	–0.025	2.135	–0.814	1.233	0.011	–0.891	–0.728	–0.162	–0.003	–0.808
OFES2	0.007	1.066	–0.113	1.383	–0.020	–0.783	–1.365	–0.100	0	–0.061

ATLANTIC OCEAN (0–300 m)

	OHC	HF	VHA	P1	P5	P6	P10	Residual
OFES1	0.032	0.184	–0.445	–0.823	0.891	–0.085	–0.440	0.749
OFES2	–0.014	–0.036	0.005	–0.665	0.783	–0.051	–0.388	0.338

INDIAN OCEAN (0–300 m)

	OHC	HF	VHA	P1	P2	P3	P7	P8	Residual
OFES1	0.026	0.195	–0.639	0.823	–0.038	–1.233	0.728	0.162	0.028
OFES2	0.035	–0.534	–2.091	0.665	–0.012	–1.383	1.365	0.100	1.926

Middle layer

~~There were no significant differences between the OFES1 and OFES2 in t~~The horizontal and vertical heat transport~~transports~~ in the middle layer (300–700 m) of the Pacific Ocean (Tab. 3), estimated by OFES1 and OFES2, displayed no significant difference. It can be seen that the ITF~~T~~ was weak for this ~~depth~~ deeper layer, and ~~its~~ the differences in the results from ~~between the~~ OFES1 and OFES2 were~~was~~ small (0.084 W/m^2). However, there was heat ~~was~~ advected or diffused from the upper layer (at 300 m, the top face of the middle ocean layer). There was a difference of approximately~~around~~ 0.747 W/m^2 in the VHD at a depth of 300 m in the Pacific Ocean and a difference of 0.701 W/m^2 in the VHA. All these results~~together~~ led us to infer a VHD difference of 1.295 W/m^2 at a depth of 700 m in the Pacific Ocean, with more heat diffusing~~was diffused~~ downward in the OFES1.

In the Atlantic Ocean, the average~~averaged~~ OHC trend, estimated by OFES1, w~~w~~as positive ~~in~~. It was, however, ~~the OFES1 but~~ negative in ~~the~~ OFES2, with a difference~~different~~ of~~by~~ 0.129 W/m^2. A VHA of –1.585 W/m^2 was calculated for ~~the~~ OFES2, which was 32% stronger than that for ~~the~~ OFES1. Additionally, more heat was lost through ~~the~~ P1 into the Indian Ocean, and more heat was advected into the Atlantic Ocean through the Drake Passage in the OFES1. Differences also existed in the heat advection between the Atlantic Ocean~~,~~ and the Southern Ocean (P6) and the Arctic (P10) Oceans. The vertical heat transport (VHA + VHD) at ~~the~~ 300 m in~~of~~ the Atlantic Ocean (Tab. 2)~~-~~was close between~~from~~ the two OFES data. The ~~resulting~~ inferred VHD ~~through~~ at a~~the~~ depth of 700 m in the Atlantic Ocean was upward in both datasets, ~~but~~ although it was stronger by 0.393 W/m^2 ~~stronger~~ in the OFES2.

—The average~~averaged~~ OHC trend in the Indian Ocean was weakly negative for~~in~~ both ~~the~~ OFES1 and OFES2. ~~OFES2 demonstrated that the heat advected downward at a depth of 700 m was increased by 0.142 W/m^2~~There was more heat (by 0.142 W/m^2)~~was~~ advected downward at a depth of 700 m in the OFES2. Horizontally, 0.121 W/m^2 more heat was acquired from the Atlantic Ocean (through ~~the~~ P1) in the OFES1, ~~but~~ however, there were negligible~~neglectable~~ differences in the lateral heat transport through the other~~others~~ passages connecting the Indian Ocean with ~~the~~ other basins. The time-averaged VHD at 700 m in the Indian Ocean was 0.423 W/m^2 in ~~the~~ OFES1 and 1.083 W/m^2 in ~~the~~ OFES2.

—To summarize, the notable cooling trend in the Pacific and Atlantic Oceans (Fig.3), determined ~~from the~~using OFES2 was~~came~~ mainly generated from ~~the~~ vertical heat transport (VHA + VHD) processes. For example, there was a net upward heat advection at 300 m in the OFES2 Atlantic Ocean and a stronger downward heat advection at 700 m~~,~~. ~~as~~ As a result, more heat was lost vertically in the middle layer of the OFES2 Atlantic Ocean compared to the OFES1 Atlantic Ocean.

Table 3. As for Tab. 2 but for the middle layer (300–700 m). VHA is at a depth of 700 m.

PACIFIC OCEAN (300–700 m)								
	OHC	VHA	P3	P4	P5	P7	P8	P9	Residual
OFES1	0.017	–0.096	1.208	–0.026	–1.056	0.044	0	0	–1.679
OFES2	–0.034	–0.084	1.247	–0.030	–0.917	–0.040	0	0	–0.384
ATLANTIC OCEAN (300–700 m)									
	OHC	VHA	P1	P5	P6	P10	Residual		
OFES1	0.037	–1.203	–0.770	1.056	0.056	–0.057	1.260		
OFES2	–0.092	–1.585	–0.649	0.917	0.017	–0.102	1.653		
INDIAN OCEAN (300–700 m)									
	OHC	VHA	P1	P2	P3	P7	P8	Residual	
OFES1	–0.010	–0.519	0.770	–0.043	–1.208	–0.044	0	0.423	
OFES2	–0.013	–0.661	0.649	–0.043	–1.247	0.040	0	1.083	

Lower layer

Consistent with Fig. 4, the OFES2 showed cooling in the bottom (700–2000 m) layer of each basin, ~~but~~ however, the OFES1 showed~~an~~ overall warming (Tab. 4). In the Pacific Ocean, the VHA at 2000 m was downward and ~~of~~ had a similar magnitude in the two OFES datasets. Owing~~Due~~ to the vertical coherence of the ACC, there was intense eastward heat advection through ~~the~~ P3 and P5, even below 700 m, with the OFES2 showing ~~greater~~ higher advection. The horizontal heat advection through ~~the~~ P4 and P7 was relatively weak, ~~but again~~although it was still larger in ~~the~~ OFES2. For example, the MHA passing through ~~the~~ P7 was more than two times larger in the OFES2. In fact, more heat advected southward into the Indian Ocean through the ITF, which was found in all the ocean layers (~~the~~ OFES1 showed a weakly northward heat advection in the middle layer). As a result of these differences~~,~~ and the estimated VHA and VHD at a depth of 700 m, we calculated a significant difference of approximately 1.252 W/m^2 in the VHD (in the downward direction) between the two OFES datasets at a depth of 2000 m in the Pacific Ocean of approximatelyaround 1.252 W/m^2 in the downward direction.

Unlike at 2000 m in the Pacific Ocean, OFES2 reflected that there was a much significantly stronger downward heat advection at 2000 m in the OFES2 Atlantic Ocean. The dominant horizontal heat advections were through the P1 and P5, with the OFES2 showing stronger heat advection at both the two passages. We calculated a downward heat diffusion at a depth of 2000 m of 0.216 W/m^2 in the OFES1 Atlantic Ocean and an upward VHD of 0.383 W/m^2 in the OFES2 Atlantic Ocean.

In the Indian Ocean, the calculated that the downward heat advection was twicetwo astimes strongstronger in the OFES1; there were also some moderate differences in the horizontal heat advection. The resulting VHD at 2000 m was upward in both the OFES1 and OFES2, but although it was much greater (by 0.455 W/m^2) in the latter.

InTo summarysummarize, the differences in the lateral heat advection through the major passages P1–P10 in the lower layer werewas small, and the major drivers of the examined OHC differences between the OFES1 and OFES2 came were generated largely from the vertical heat transport (VHA + VHD), similar to the situation in the middle layer.

Table 4. As for Tab. 2 but for the lower layer (700–2000 m). VHA is at a depth of 2000 m.

PACIFIC OCEAN (700–2000 m)									
	OHC	**VHA**	**P3**	**P4**	**P5**	**P7**	**P8**	**P9**	**Residual**
OFES1	0.058	−0.126	0.951	−0.047	−1.120	−0.035	0	0	−1.341
OFES2	−0.037	−0.105	1.146	−0.080	−1.294	−0.082	0	0	−0.089
ATLANTIC OCEAN (700–2000 m)									
	OHC	**VHA**	**P1**	**P5**	**P6**	**P10**	**Residual**		
OFES1	0.014	−0.029	−0.974	1.120	0.066	0.105	–0.216		
OFES2	−0.013	−0.536	−1.059	1.294	0.003	−0.031	0.383		
INDIAN OCEAN (700–2000 m)									
	OHC	**VHA**	**P1**	**P2**	**P3**	**P7**	**P8**	**Residual**	
OFES1	0.007	−0.241	0.974	−0.033	−0.951	0.035	0	0.126	
OFES2	−0.018	−0.120	1.059	−0.052	−1.146	0.082	0	0.581	

4 Conclusions and Discussion

In this studypaper, we estimated the OHC from based on two eddy-resolution hindcast simulations, OFES1 and OFES2, with a major focus on estimating their differences. The global observation-based dataset EN4 acted as a reference. The main findings of this study arewere as follows:.

—1. Multi-decadal warming was clearly seen evinced in most of the global ocean (0–2000 m), especially in the EN4 and OFES1 dataset. The warming was mainly dominantly manifested as deepening of the neutral density surfaces (HV component), with a changes along the neutral surfaces (SP component) of regional importance.

—2. Significant differences in the OHC (or potential temperature) were found between the OFES1 and OFES2; the major causes for these were fourfold. -FirstFirstly, there was generally morethe net surface HFheat flux in in the OFES21 was generally higherweaker. SecondSecondly, the ITF was almost twicetwo astimes strongstronger in the OFES2, especially in the top 300 m. ThirdThirdly, the differences in the intensity of the VHAvertical heat advection were large, particularly at a depth of 300 m in the Indian Ocean. Finally, remarkable differences in the vertical heat diffusion were inferred.

—3. Overall, the global and basin-integrated OHC estimates over the 57-years period yearsfor the period 1960–2016 are generallywere -reasonable in for the top 700 m upon considering -ofin the OFES1 results. Below 700 m, multi-decadal climate changes derived from the OFES1 need careful evaluations, although even though the estimates of global OHC estimate between 700 –2000 m is are highly correlated with observations. The notable differences between the OFES2 and EN4 suggestsuggested that attention is clearly warranted when making conclusionswhile concluding on multi-decadal climate changes based on the OFES2.

—Although we have detailed the OHC differences between the OFES1 and OFES2, and also analyzedanalysed the horizontal and vertical heat transporttransports in an attempt to understand the causes of these differences, more further work is needed required to for improveimproving this field. FirstFirstly, a direct calculation of the vertical heat diffusion iswas desirable to obtainhave a more reliable and accurate comparison between the two datasetsOFES. In addition, decomposing the vertical heat diffusion into tidal mixing and mixed-layer vertical mixing is also an interesting topic, and may help to isolate the effects of tidal mixing on in the ocean state. In additionBesides, we expect to see a detailed comparison of the wind stress from these two datasets over this the 57-year period years. This is inspired by the work of Kutsuwada et al. (2019) and our detection of the large differences in the VHAvertical heat advection. Considering the apparent differences inof the SP between the OFES2 and the other two datasets, a comprehensive comparison of salinity between both the OFES1 and OFES2, along with observations, waswere required. This helped the community to determine their choice of datasets for their own research purposes.

—One may argue that being notthe inability to well spun-up completely may be the majorcould be the likely cause for the identified differences between the OFES2 andwith othersother datasets, since that the OFES1 followed a 50-year climatological simulation but OFES did not. This is likely to be thea cause. However, large differences between the two OFES datasets remain can be seen in the temporal evolution of the global and basin OHCs, even during the last two decades. In addition, for example, **S2020** found that the Azores Current was simulated in the OFES2 in the initial two decades, however, it but disappeared after 1970. This, to some extent, weakensweaken the spin-up argument, but although it does not rule out the possibility completely. The OFES2 was not expected to be highly sensitive to the spin-up issue, as because the starting conditions are from OFES1. That said, there were indeed some improvements in the OFES2 for during the recent decades, for example, from toover 2005-2016 (not shown here). Two potential explanations are as follows: Firstfirstly, the model was full completelywell spun-up after a couple of decades of integration; second~~secondly~~, improvements in~~of~~ the reanalysis of atmospheric forcing data contributed to ~~the~~ improvements in simulation~~ improvements~~.

As mentioned above, ~~the~~ results based on EN4 should not be considered~~taken~~ as the ~~the most ideal dataset~~*truth*. ~~Factors~~ Several factors such as mapping methods and data ~~ingested ingestion~~assimilated impact the resulting quality of the~~those~~ ~~objective-analysis~~observational-based products, and ~~may~~ might consequently alter our conclusions~~ here consequently~~. As a preliminary test of robustness, we compared the temporal evolution of the OHC (Fig. S10)~~,~~ and the spatial patterns~~pattern~~ of the long-term potential temperature trend (Fig. S11) ~~between~~ determined using EN4 and two ~~more~~ datasets, G10 and IAP. G10 is the most up-to-date~~up to date~~ version of EN4 datasets (EN4.2.2) with ~~bias~~ bias-corrected following Gouretski and Reseghetti (2010),~~;~~ and IAP is the dataset from the Institute of Atmospheric Physics (Cheng and Zhu, 2016). The primary difference between ~~the~~ EN4 (~~bias~~ bias-corrected following Levitus et al. (2009)) and G10 lies in the bias correction methods, whereas IAP differs from EN4 in assimilated datasets, ~~bias correction, and~~ mapping methods, and among others. The ~~high~~ large similarities between EN4 and G10 suggest that the different correction methods do not lead to notable differences in the resulting state estimates~~estimate~~. On the other hand, there were~~do exist~~ some differences between the IAP and both EN4 and G10. This may indicate that the applied mapping method ~~applied~~ causes~~cause~~ some discrepancies among different oceanic products, which is consistent with Cheng and Zhu (2016).

Finally, in absence of any observation-based constraints, the OFES products, especially the OFES1, have captured~~did capture~~ some of the warming and cooling trends shown by ~~the~~ EN4 and in the literature~~, despite their having no observation-basedobservational-based constraints~~. However, ~~the~~ clear differences between the two OFES datasets and ~~the~~ EN4 suggest the importance of observational data in improving the performance of ~~the~~ hindcast ~~performance~~. The significant differences in the vertical heat diffusion between the two OFES datasets also suggest that special attention should be given to the validation of the vertical mixing scheme in future ocean mode~~l~~ling.

Author contributions: F.L conceived the study. All authors contributed to the details of study design. F.L conducted the calculations and analysis. F.L drafted the manuscript; Z.L and X.H.W improved the writing.

Acknowledgements: This is publication No. 87 of the Sino-Australian Research Consortium for Coastal Management (previously the Sino-Australian Research Centre for Coastal Management). This work was supported by the Key Special Project for Introduced Talents Team of the Southern Marine Science and Engineering Guangdong Laboratory (Guangzhou; GML2019ZD0210). The authors thank Dr. Peter McIntyre for improving the manuscript. The authors acknowledge public access to the data used in this paper from the UK Meteorological Office and the JAMSTEC. Constructive comments from the editor and two anonymous reviewers greatly improved the manuscript.

Code and data availability: OFES1 and OFES2 are based on the MOM3, available at https://github.com/mom-ocean/MOM3. Code for decomposing the potential temperature: http://www.teos-10.org/software.htm. Original EN4 data: https://www.metoffice.gov.uk/hadobs/en4/download-en4-2-1.html. Original OFES1 temperature and salinity data: http://apdrc.soest.hawaii.edu/dods/public_ofes/OfES/ncep_0.1_global_mmean. Due to a data security incident, access to the OFES2 data has been temporarily suspended. The data and codes (including the publically available scripts for completion) needed to reproduce the results of this paper are archived on Zenodo (https://doi.org/10.5281/zenodo.5205444). The archived data are annual mean values calculated from the original data.

References

Abraham, J. P., Reseghetti, F., Baringer, M., Boyer, T., Cheng, L., Church, J., Domingues, C., Fasullo, J. T., Gilson, J., Goni, G., Good, S., Gorman, J. M., Gouretski, V., Ishii, M., Johnson, G. C., Kizu, S., Lyman, J., MacDonald, A., Minkowycz, W. J., Moffitt, S. E., Palmer, M., Piola, A., Trenberth, K. E., Velicogna, I., Wijffels, S., and Willis, J.: A review of global ocean temperature observations: implications for ocean heat content estimates and climate change, Rev. Geophys., 51, 450-483, doi.org/10.1002/rog.20022, 2013.

AchutaRao, K. M., Ishii, M., Santer, B. D., Gleckler, P. J., Taylor, K. E., Barnett, T. P., Pierce, D. W., Stouffer, R. J., and Wigley, T. M. L.: Simulated and observed variability in ocean temperature and heat content, Proc. Natl. Acad. Sci., 104,10768-10773, doi.org/10.1073/pnas.0611375104, 2007.

Allison, L. C., Roberts, C. D., Palmer, M. D., Hermanson, L., Killick, R. E., Rayner, N. A., Smith, D. M., and Andrews, M. B.: Towards quantifying uncertainty in ocean heat content changes using synthetic profiles, Environ. Res. Lett., 14, 084037, doi.org/10.1088/1748-9326/ab2b0b, 2019.

Balmaseda, M. A., Trenberth, K. E., and Källén, E.: Distinctive climate signals in reanalysis of global ocean heat content, Geophys. Res. Lett., 40, 1754-1759, doi.org/10.1002/grl.50382, 2013.

Bindoff, N. L., and McDougall, T. J.: Diagnosing climate change and ocean ventilation using hydrographic data, J. Phy. Oceanogr., 24, 1137-1152, doi.org/10.1175/1520-0485(1994)024<1137:DCCAOV>2.0.CO;2, 1994.

Carton, J. A., Chepurin,G. A. and Chen, L.: SODA3: A New Ocean Climate Reanalysis, *J. Climate.*, 31, 6967-6983, https://doi.org/10.1175/JCLI-D-18-0149.1, 2018.

Banks, H. T., and Gregory, J. M.: Mechanisms of ocean heat uptake in a coupled climate model and the implications for tracer based predictions of ocean heat uptake, Geophys. Res. Lett., 33, L07608, https://doi.org/10.1029/2005GL025352, 2006.

Carton, J. A., Chepurin, G., A. and Chen, L.: SODA3: A New Ocean Climate Reanalysis, J. Climate., 31, 6967-6983, https://doi.org/10.1175/JCLI-D-18-0149.1, 2018.

Carton, J. A., Penny, S. G., and Kalnay, E.: Temperature and salinity variability in the SODA3, ECCO4r3, and ORAS5 ocean reanalyses, 1993–2015, J. Climate., 32, 2277-2293, doi.org/10.1175/JCLI-D-18-0605.1, 2019.

Chen, X., Yan, Y., Cheng, X., and Qi, Y.: Performances of seven datasets in presenting the upper ocean heat content in the South China Sea, Adv. Atmos. Sci., 30, 1331-1342, doi.org/10.1007/s00376-013-2132-1, 2013.

Cheng, L., Trenberth, K. E., Palmer, M. D., Zhu, J., and Abraham, J.: Observed and simulated full-depth ocean heat content changes for 1970–2005, Ocean Sci., 12, 925-935, doi.org/10.5194/os-12-925-2016, 2016.

Cheng, L., and Zhu, J.: Artifacts in variations of ocean heat content induced by the observation system changes. Geophys. Res. Lett., 41, 7276-7283, https://doi.org/10.1002/2014GL061881, 2014.

Cheng, L., and Zhu, J.: Benefits of CMIP5 Multimodel Ensemble in Reconstructing Historical Ocean Subsurface Temperature Variations. J. Climate., 29(15), 5393–5416, https://doi.org/10.1175/JCLI-D-15-0730.1, 2016.

Cheng, L., Abraham, J., Goni, G., Boyer, T., Wijffels, S., Cowley, R., Gouretski, V., Reseghetti, F., Kizu, S., Dong, S., Bringas, F., Goes, M., Houpert, L., Sprintall, J., and Zhu, J.: XBT Science: Assessment of Instrumental Biases and Errors. Bull. Am. Meteorol. Soc., 97(6), 924–933, https://doi.org/10.1175/BAMS-D-15-00031.1, 2016.

Church, J. A., White, N. J., and Arblaster, J. M.: Significant decadal-scale impact of volcanic eruptions on sea level and ocean heat content, Nature, 438, 74-77, doi.org/10.1038/nature04237, 2005.

Curry, R., Dickson, B. and Yashayaev, I.: A change in the freshwater balance of the Atlantic Ocean over the past four decades. Nature, 426**,** 826-829, https://doi.org/10.1038/nature02206, 2003.

Desbruyères, D., McDonagh, E. L., King, B. A., and Thierry, V.: Global and Full-Depth Ocean Temperature Trends during the Early Twenty-First Century from Argo and Repeat Hydrography, J. Climate., 30, 1985-1997, doi.org/10.1175/JCLI-D-16-0396.1, 2017.

Desbruyeres, D., Purkey, S. G., Mcdonagh, E. L., Johnson, G. C. and King, B. A.: Deep and abyssal ocean warming from 35 years of repeat hydrography. Geophys. Res. Lett., 43, 10356-10365, doi.org/10.1002/2016GL070413, 2016.

Dong, S., Garzoli, S., and Baringer, M.: The role of interocean exchanges on decadal variations of the meridional heat transport in the South Atlantic, J. Phys. Oceanogr., 41, 1498-1511, doi.org/10.1175/2011JPO4549.1, 2011.

Durack, P. J., Gleckler, P. J., Landerer, F. W., and Taylor, K. E.: Quantifying underestimates of long-term upper-ocean warming, Nat. Climate Change., 4, 999-1005, https://doi.org/10.1038/nclimate2389, 2014.

Du, Y., Qu, T., Meyers, G., Masumoto, Y., and Sasaki, H.: Seasonal heat budget in the mixed layer of the southeastern tropical Indian Ocean in a high-resolution ocean general circulation model, J. Geophys. Res. Oceans., 110, C04012, doi.org/10.1029/2004JC002845, 2005.

Emery, W.: Water Types and Water Masses, Encyclopedia of Ocean Sciences, 4, 3179-3187, doi.org/10.1006/rwos.2001.0108, 2001.

Ernst, W. G.: *Earth systems: processes and issues.* Cambridge University Press, 2000.

Forget, G., Campin, J.-M., Heimbach, P., Hill, C. N., Ponte, R. M., and Wunsch, C.: ECCO version 4: an integrated framework for non-linear inverse modeling and global ocean state estimation, Geosci. Model Dev., 8 (10), 3071–3104, doi:10.5194/gmd-8-3071-2015, 2015.

Fyfe, J.: Southern Ocean warming due to human influence, Geophys. Res. Lett., 33, L19701, 10.1029/2006GL027247, 2006.

Gleckler, P. J., Santer, B. D., Domingues, C. M., Pierce, D. W., Barnett, T. P., Church, J. A., Taylor, K. E., Achutarao, K., Boyer, T. P., and Ishii, M.: Human-induced global ocean warming on multidecadal timescales, Nat. Climate Change., 2, 524-529, doi.org/10.1038/nclimate1553, 2012.

Good, S. A., Martin, M., and Rayner, N. A.: EN4: Quality controlled ocean temperature and salinity profiles and monthly objective analyses with uncertainty estimates, J. Geophys. Res. Oceans., 118, 6704-6716, doi.org/10.1002/2013JC009067, 2013.

Gouretski, V., and Reseghetti, F.: On depth and temperature biases in bathythermograph data: Development of a new correction scheme based on analysis of a global ocean database. Deep Sea Res. Part I Oceanogr., 57(6), 812–833, https://doi.org/10.1016/j.dsr.2010.03.011, 2010.

Häkkinen, S., Rhines, P. B. and Worthen, D. L.: Heat content variability in the North Atlantic Ocean in ocean reanalyses, Geophys. Res. Lett., 42**,** doi.org/10.1002/2015GL063299, 2901-2909, 2015.

Häkkinen, S., Rhines, P. B., and Worthen, D.: Warming of the global ocean: Spatial structure and water-mass trends, J. Climate., 29, 4949-4963, doi.org/10.1175/JCLI-D-15-0607.1, 2016.

IPCC.: Climate Change 2013: The Physical Science Basis. Cambridge University Press, 1535pp., doi:10.1017/CBO9781107415324, 2013.

Jackett, D. R., and McDougall, T. J.: A neutral density variable for the world's oceans, J. Phys. Oceanogr., 27, 237-263, doi.org/10.1175/1520-0485(1997)027<0237:ANDVFT>2.0.CO;2, 1997.

Jayne, S. R., and Laurent, L. C. St.: Parameterizing tidal dissipation over rough topography, Geophys. Res. Lett., 28, 811-814, doi.org/10.1029/2000GL012044, 2001.

Johnson, G. C., Purkey, S. G., Zilberman, N. V., and Roemmich, D. Deep Argo Quantifies Bottom Water Warming Rates in the Southwest Pacific Basin. Geophysical Research Letters, 46(5), 2662–2669, doi.org/10.1029/2018GL081685, 2019.

Kalnay, E., Kanamitsu, M., Kistler, R., Collins, W., Deaven, D., Gandin, L., Iredell, M., Saha, S., White, G., Woollen, J., Zhu, Y., Chelliah, M., Ebisuzaki, W., Higgins, W., Janowiak, J., Mo, K. C., Ropelewski, C., Wang, J., Leetmaa, A., Reynolds, R., Jenne, R., and Joseph, D.: The NCEP/NCAR 40-year reanalysis project, B. Am. Meteorol. Soc., 77, 437-472, doi.org/10.1175/1520-0477(1996)077<0437:TNYRP>2.0.CO;2, 1996.

Kutsuwada, K., Kakiuchi, A., Sasai, Y., Sasaki, H., Uehara, K., and Tajima, R.: Wind-driven North Pacific Tropical Gyre using high-resolution simulation outputs, J. Oceanogr., 75, 81-93, 10.1007/s10872-018-0487-8, 2019.

Large, W. G., McWilliams, J. C., and Doney, S. C.: Oceanic vertical mixing: A review and a model with a nonlocal boundary layer parameterization, Rev. Geophys., 32, 363-403, doi.org/10.1029/94RG01872, 1994.

Lee, S., Park, W., Baringer, M. O. A., Gordon, L., Huber, B. A., and Liu, Y.: Pacific origin of the abrupt increase in Indian Ocean heat content during the warming hiatus, Nature Geosci., 8, 445-449, doi.org/10.1038/ngeo2438, 2015.

Levitus, S., Antonov, J. I., Boyer, T. P., Baranova, O., Garcia, H. E., Locarnini, R. A., Mishonov, A. V., Reagan, J. R., Seidov, D., and Yarosh, E. S.: World ocean heat content and thermosteric sea level change (0–2000 m), Geophys. Res. Lett., 39, 1955-2010, doi.org/10.1029/2012GL051106, 2012.

Liang, X., Piecuch, C. G., Ponte, R. M., Forget, G., Wunsch, C., and Heimbach, P.: Change of the global ocean vertical heat transport over 1993–2010, J. Climate., 30, 5319-5327, doi.org/10.1175/JCLI-D-16-0569.1, 2017.

Liang, X., Liu, C. R., Ponte, M. and Chambers, D. P.: A Comparison of the Variability and Changes in Global Ocean Heat Content from Multiple Objective Analysis Products During the Argo Period, J. Climate., 1-47, doi.org/10.1175/JCLI-D-20-0794.1, 2021.

Liu, C., Liang, X., Chambers, D. P. and Ponte, R. M.: Global Patterns of Spatial and Temporal Variability in Salinity from Multiple Gridded Argo Products, J. Climate., 33, 8751-8766, https://doi.org/10.1175/JCLI-D-20-0053.1, 2020.

Liu, M., and T. Tanhua.: Water masses in the Atlantic Ocean: characteristics and distributions, Ocean Sci., 17, 463-486, doi.org/10.5194/os-17-463-2021, 2021.

Noh, Y., and Kim, H. J.: Simulations of temperature and turbulence structure of the oceanic boundary layer with the improved near-surface process, J. Geophys. Res. Oceans., 104, 15621-15634, doi.org/10.1029/1999JC900068, 1999.

O'Connor, B. M., Fine, R. A. and Olson, D. B.: A global comparison of subtropical underwater formation rates, Deep Sea Research Part I: Oceanographic Research Papers, 52, 1569-1590, doi.org/10.1016/J.DSR.2005.01.011, 2005.

Palmer, M. D., Mcneall, D. J., and Dunstone, N. J.: Importance of the deep ocean for estimating decadal changes in Earth's radiation balance, Geophys. Res. Lett., 38, L13707, doi.org/10.1029/2011GL047835, 2011.

Pierce, D. W., Barnett, T. P., Achutarao, K., Gleckler, P. J., Gregory, J. M., and Washington, W. M.: Anthropogenic warming of the oceans: Observations and model results, J. Climate., 19, 1873-1900, doi.org/10.1175/JCLI3723.1, 2006.

Sasaki, H., Sasai, Y., Kawahara, S., Furuichi, M., Araki, F., Ishida, A., Yamanaka, Y., Masumoto, Y., and Sakuma, H.: A series of eddy-resolving ocean simulations in the world ocean-OFES (OGCM for the Earth Simulator) project, Oceans '04 MTS/IEEE Techno-Ocean '04 (IEEE Cat. No. 04CH37600) 3, 1535-1541, 2004.

Sasaki, H., Kida, S., Furue, R., Nonaka, M., and Masumoto, Y.: An Increase of the Indonesian Throughflow by Internal Tidal Mixing in a High-Resolution Quasi-Global Ocean Simulation, 45, 8416–8424, 2018. doi.org/10.1029/2018GL078040.

Sasaki, H., Kida, S., Furue, R., Aiki, H., Komori, N., Masumoto, Y., Miyama, T., Nonaka, M., Sasai, Y., and Taguchi, B.: A global eddying hindcast ocean simulation with OFES2, Geosci. Model Dev., 13, 3319-3336, doi.org/10.5194/gmd-13-3319-2020, 2020.

Smith, D. M., Allan, R.P., Coward, A.C., Eade, R., Hyder, P., Liu, C., Loeb, N.G., Palmer, M.D., Roberts, C.D. and Scaife, A.A.: Earth's energy imbalance since 1960 in observations and CMIP5 models, Geophys. Res. Lett., 42, 1205-1213, doi.org/10.1002/2014GL062669, 2015.

Spence, P., Saenko,O. A., Sijp, W., and England, M.: The role of bottom pressure torques on the interior pathways of North Atlantic deep water, J. Phys. Oceanogr., 42, 110-125, doi.org/10.1175/2011JPO4584.1, 2012.

St. Laurent, L. C., Simmons, H. L., and Jayne, S. R.: Estimating tidally driven mixing in the deep ocean, Geophys. Res. Lett., 29, 21-21–21-24, doi.org/10.1029/2002GL015633, 2002.

Talley, L. D.: Shallow, Intermediate, and Deep Overturning Components of the Global Heat Budget, J. Phys. Oceanogr., 33, 530-560, https://doi.org/10.1175/1520-0485(2003)033<0530:SIADOC>2.0.CO;2, 2003.

Trenberth, K. E., Fasullo, J. T., Von Schuckmann, K., and Cheng, L.: Insights into Earth’s energy imbalance from multiple sources, J. Climate., 29, 7495-7505, doi.org/10.1175/JCLI-D-16-0339.1, 2016.

Tsujino, H., Urakawa, S., Nakano, H., Small, R. J., Kim, W. M., Yeager, S. G., Danabasoglu, G., Suzuki, T., Bamber, J. L., Bentsen, M., Böning, C. W., Bozec, A., Chassignet, E. P., Curchitser, E., Boeira Dias, F., Durack, P. J., Griffies, S. M., Harada, Y., Ilicak, M., Josey, S. A., Kobayashi, C., Kobayashi, S., Komuro, Y., Large, W. G., Le Sommer, J., Marsland, S. J., Masina, S., Scheinert, M., Tomita, H., Valdivieso, M., and Yamazaki, D.: JRA-55 based surface dataset for driving ocean-sea-ice models (JRA55-do), Ocean Model., 130, 79-139, doi.org/10.1016/j.ocemod.2018.07.002, 2018.

Von Schuckmann, K., Palmer, M. D., Trenberth, K. E., Cazenave, A., Chambers, D. P., Champollion, N., Hansen, J., Josey, S. A., Loeb, N. G., and Mathieu, P. P.: An imperative to monitor Earth's energy imbalance, Nat. Climate Change., 6, 138-144, doi.org/10.1038/nclimate2876, 2016.

Wang, G., Cheng, L., Abraham, J., and Li, C.: Consensuses and discrepancies of basin-scale ocean heat content changes in different ocean analyses, Clim. Dyn., 50, 2471-2487, doi.org/10.1007/s00382-017-3751-5, 2018.

Wang, X. H., Bhatt, V., and Sun, Y.-J.: Study of seasonal variability and heat budget of the East Australian Current using two eddy-resolving ocean circulation models, Ocean. Dyn., 63, 549-563, doi.org/10.1007/s10236-013-0605-5, 2013.

Wunsch, C.: The decadal mean ocean circulation and Sverdrup balance, J. Mar. Res., 69, 417-434, doi.org/ 10.1357/002224011798765303, 2011.

Zanna, L., Khatiwala, S., Gregory, J. M., Ison, J., and Heimbach, P.: Global reconstruction of historical ocean heat storage and transport, Proc. Natl. Acad. Sci., 116, 1126-1131, doi.org/10.1073/pnas.1808838115, 2019.

Zhang, Y., Feng, M., Du,Y. H., Phillips, E., Bindoff, N. L., and McPhaden, M. J.: Strengthened Indonesian Throughflow Drives Decadal Warming in the Southern Indian Ocean, Geophys. Res. Lett., 45, 6167-6175, doi.org/10.1029/2018GL078265, 2018.